

A Tutorial on Controlling Metasurfaces from the Network Perspective

Christos Liaskos¹, Evangelos Papapetrou², Kostas Katsalis³, Dimitrios Tyrovolas⁴, Alexandros Papadopoulos⁵, Stavros Tsimpoukis⁶, Arash Pourdamghani⁷, Max Franke⁸, Stefan Schmid⁹

^{1,2,5,6}University of Ioannina, Ioannina, Greece, emails: {cliaskos, epap, a.papadopoulos, s.tsimpoukis}@uoi.gr

³DOCOMO Euro-Labs, Munich, Germany, email: Katsalis@docomolab-euro.com

⁴University of Patras, Greece, email: dtyrovolas@upnet.gr

^{7,8,9}Technical University of Berlin, Germany, emails: {pourdamghani, m.franke, stefan.schmid}@tu-berlin.de.

Abstract—Metasurfaces have emerged as transformative electromagnetic structures for wireless communications, enabling the real-time control over wave propagation, yielding potential for improved data rates, privacy, energy efficiency and even precise environmental sensing. This tutorial offers a perspective on controlling metasurfaces by treating them as components of a larger networked system. Towards this end, we first review the physical principles of metasurfaces and their various applications, followed by an exploration of manufacturing approaches for creating these structures. Then, aligning with standard network-layer concepts, we describe the modeling of metasurfaces as wave routers, enabling us to describe systems of metasurfaces using graph theory. This approach enables the development of a performance objective framework for optimizing these systems, while classes of heuristic and path-finding-driven algorithms are discussed as practical solvers. The paper also examines the integration of metasurfaces with communication systems, by presenting their overall workflow, discussing its relation to ongoing standardization efforts, as well as defining a context for their integration to network simulators, using Omnet++ as a driving example. Finally, the paper explores future directions for research in this field, identifying graph-theoretic, standardization and integration challenges, relating to several networking disciplines, such as time-sensitive networking, age of information and scheduling. The paper also considers the potential of AI-driven applications, beyond classic data transfer objectives.

Index Terms—Metasurfaces, network theory, graphs, integration, wireless, infrastructure, optimization, modeling, simulation, 6G.

I. INTRODUCTION

In recent years, wireless networks have begun to undergo a paradigm shift, extending connectivity beyond user devices to include previously passive obstacles in the environment [1]. The enablers of this paradigm are known as metasurfaces, thin artificial materials supporting programmable interaction types with impinging wireless waves [2]. The interactions include programmable steering, focusing, absorption, phase control, and polarization manipulation.

Leveraging such functionalities in a system where planar objects have been covered with metasurfaces, denoted as Programmable Wireless Environments (PWEs) [3], has allowed for considerable performance gains in network data rates, privacy, coverage and energy efficiency. These gains result from configuring a PWE to mitigate the long-standing

degradation factors of wireless networks. Signal dissipation can be countered by wave focusing, blockage can be countered by steering waves via alternative paths, a technique which can also be exploited for improving privacy and reducing interference.

Historically, PWEs constitute the culmination of an ongoing effort to exert control over the propagation process. Preceding efforts included the use of passive relays [4], [5], large antenna arrays [6], and metasurfaces [7], evolving from coarse-grained to fine control over waves, respectively, within a strict signal processing context. In the PWE iteration, the control over wireless propagation was structured over networking principles [8]. One significant advantage of this approach is the ability to optimize metasurface systems by considering them as part of a broader network of interconnected systems and services, while adopting an OSI-compliant approach for their operation and future evolution.

However, while the introduction of metasurfaces to the discipline of wireless communications has produced significant outcomes, the multi-disciplinary nature of the field and the abundance of research output calls for a structured tutorial aimed at an audience with a networking background. To this end, this paper presents a perspective on controlling metasurfaces by treating them as nodes of a network. By leveraging concepts from network practices and graph theory, we demonstrate how this approach can provide new insights into the design, optimization, and integration of metasurfaces with existing infrastructure. Specifically, the contributions of the present paper are as follows:

- We provide the necessary prerequisites from the aspect of physics, electronics, resource utilization and the related nomenclature in a compact and self-complete manner, targeting computer and network scientists (Section II).
- Employing network-layer concepts, we detail a model for representing metasurfaces as wave routers and systems metasurfaces, i.e., PWEs, as graphs, and their physical capabilities as network functions (Section III).
- We formulate the problem of configuring PWEs for a set of users as a resource sharing optimization problem, relating to the existing concepts of network orchestration and network update consistency (Section IV).
- We discuss the integration of PWEs to existing networks

by first defining their workflow from initialization to operation, and then exploring the existing standardization landscape and its future directions (Section V).

- We provide a context for simulating PWEs using well-known network simulators, using Omnet++ as the driving example (Section VI).
- We present an exemplary, simulation-driven evaluation scenario employing PWEs in a challenging wireless optimization, involving the mitigation of Doppler spread in a factory setting (Section VII).
- We relate future challenges to existing networking directions such as time-sensitive networking, age of information, scheduling, traffic engineering and routing (Section VIII).

Notably, the merge of metasurfaces and communications has been highly prolific in terms of research outcomes in recent years. This paper is not intended as an extensive survey of these numerous efforts, but rather seeks to serve as a tutorial and a roadmap for network-layer and computer theory researchers interested in exploring the intersection of metasurfaces and their respective field.

II. BACKGROUND: FROM METASURFACE PHYSICS TO MODELING AS NETWORK COMPONENTS

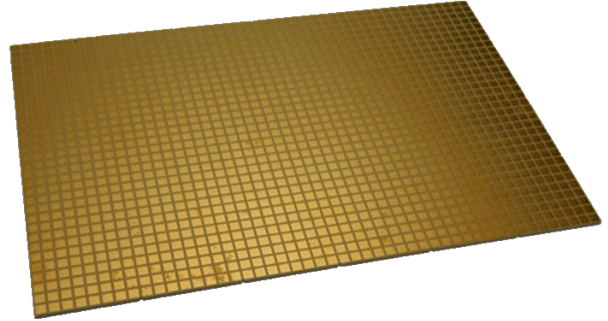
In this section we provide a short survey of how metamaterials look, are manufactured and operate from the standpoint of physics. The goal is to provide the basic foundations for understanding their network-layer modeling, which constitutes the main goal of this paper, and is provided in Section III and on.

A. Metasurfaces: A Review of Their Physical Principles and Applications

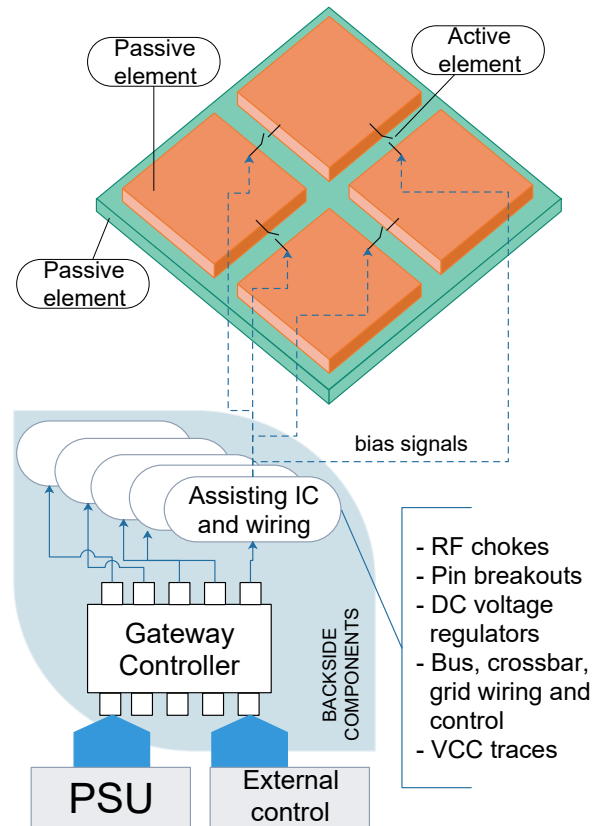
Metasurfaces, also known as 2D meta-materials or artificial surfaces, have revolutionized various fields of research and technology due to their unique electromagnetic properties and potential applications [9]. From a physical perspective, metasurfaces are engineered structures composed of periodic arrays of sub-wavelength elements that interact with incident electromagnetic waves. This section surveys the underlying physics behind metasurfaces and their practical applications, to provide a basic level of understanding required for detailing the network control aspect.

Typical appearance: Metasurfaces commonly (but not exclusively) consist of an array of a metal-on-dielectric basic design arranged in a periodic pattern [10], as shown in Fig. 1. This basic design is usually denoted as *cell* and can also comprise components with controllable impedance in the radio-frequency (RF) regime. In this case, the metasurface is deemed as *programmable* and a separate, DC-logic circuitry transfers control over the tunable impedances to an external computer. Special circuit components, known as *RF chokes*, ensure that no RF signal leaks into the DC-logic circuitry.

The dimensions of a cell is at least in the $\lambda/2$ order and, ideally, go below $\lambda/8 - \lambda/10$, λ being the wavelength of the incident electromagnetic wave, which yields a significant degree of modification potential of the reflective behavior of the



(a) Photographic sample of a $\lambda/8$ metasurface (front-side), manufactured as a printed circuit board. (EU Project VISORSURF, <https://projects.research-and-innovation.ec.europa.eu/en/projects/success-stories/all/hypersurfaces-control-electromagnetic-energy-app>).



(b) Front-side schematic close up and backside components.

Figure 1: Typical constituents of a metasurface.

metasurface [11]. This includes achieving negative refractive index, perfect absorption, and customized scattering. These properties arise from the interaction between the incident wave, the metasurface's periodic elements, and the chosen impedance values, which can either reinforce or cancel out specific frequency components of the wave.

Operating Principle: In general, a metasurface operates by controlling surface currents across its structure created via induction from impinging waves, as shown in Fig 2 [12].

Table I: Terminology

Term	Definition
Software-Defined Metamaterial (SDM)	General term for all planar and non-planar metamaterials that can manipulate impinging electromagnetic waves following software commands, to control wireless signal propagation.
Metasurface	The most advanced design approach for planar SDMs at the physical layer (i.e., not encompassing software or control circuitry). Metasurfaces enable the manipulation of electromagnetic waves in almost any desired way.
Reconfigurable Intelligent Surface (RIS)	A specific SDM technology, that employs reflectarrays at the physical layer, offering a subset of the metasurface capabilities.
Tile	Any planar SDM, when deployed in batches to cover a large surface, such as a wall.
Programmable Wireless Environment (PWE)	A 3D space whose inner surfaces are covered with SDMs, either in part or in full, allowing for the propagation of wireless waves to be programmable by assigning EM Functions to tiles.
Metasurface codebook	A template describing an EM manipulation type and its parameters. (E.g., STEER a wave, by defining incoming and reflection directions).
Metasurface codebook	A database containing the circuit-level metasurface-internal instructions to obtain every supported .

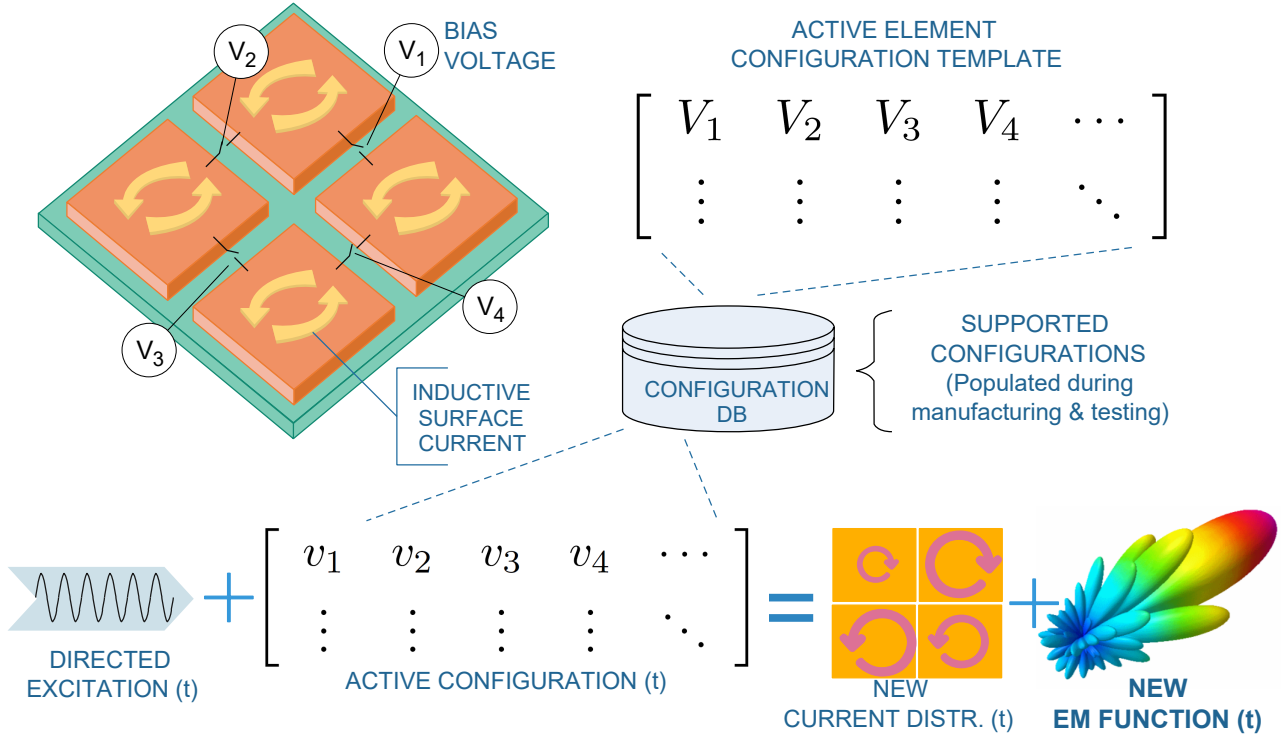


Figure 2: Metasurface functionality: Incident EM waves cause unit cells to respond in a controlled manner for creating a specific EM response, dictated by the selected state of active elements and the resulting inductive surface currents. The cell-level engineered response can be time-variant and follows a predetermined design goal such as directing reflection towards a custom angle. The configuration DB, also known as codebook, defines a format for a whole-tile configuration entries, $[V]$, valid for a given tile design, and specific entries, each corresponding to an EM response/function, $[v]$.

The total electromagnetic response is calculated based on the emitted field resulting from these currents. Engineering of surface current dynamics involves considering direct, inductive currents on the passive parts of the cells, currents wirelessly induced by neighboring cells, and the current flow controlled by the tunable impedance circuit elements. This can be conceptualized as a network of input and output antennas connected through custom topologies using switch elements, where incident waves are routed according to switch element states before exiting. A departing wave of any specific form has the equivalent surface current distribution that creates it,

which in turn can manifest by transforming the inductive waves via the circuit elements.

This workflow, as shown in Fig 2, can also be a time-variant process. The metasurface can change its response while the same wave impinges upon it, e.g., in order to steer it to another direction, or when the impinging wave changes, in order to adapt to it. Moreover, the time-scale of this time-variant behavior can be larger than λ or smaller than it. In the latter case, the impinging signal remains intact and is redirected to another direction, or is absorbed. In the former case, the metasurface *alters* the impinging signal. For instance, consider

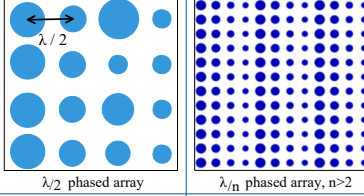
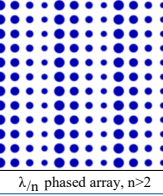
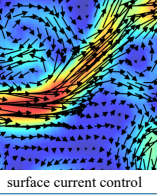
Term	RIS	Holographic RIS	Metasurface
Operating Principle	 $\lambda/2$ phased array	 λ/n phased array, $n > 2$	
Applications	Theoretical modeling Exploration of performance bounds Probabilistic channel engineering	Practical beam steering Object localization and sensing SNR engineering	Deterministic channel control Precise 4D imaging Precise EM vector field engineering

Figure 3: Overview of the usual metasurface-related nomenclature and their main applications in the literature.

a single sinusoid of wavelength λ as the impinging wave. If the metasurface alternates between steering and absorption per $\lambda/2$, the response would be an ON-OFF keying-modulated steered signal.

Nomenclature: This general operating principle of metasurfaces as manipulators of inductive surface currents is commonly simplified, exchanging performance for ease of modeling and/or manufacturing. In particular, metasurfaces are oftentimes treated as synonymous to antenna arrays, where each cell is an isolated or coupled phase shifter, disallowing the direct flow of inductive current between neighboring cells [13], [14]. This electric isolation is also enforced in the z-axis, where phase shifter arrays are stacked for better performance, while metamaterials—the 3D counterpart of metasurfaces—remain fully electrically connected in the vertical direction as well. These simplifications are typically introduced to enable analytically tractable channel models and formulations, rather than to faithfully represent the full extend of the electromagnetic capabilities of metasurfaces.

This simplification has often appeared under multiple—and often changing—naming conventions in the literature, such as reconfigurable intelligent surfaces (RIS) and holographic RIS (HRIS), denoting sparser-to-denser phased arrays, as shown in Fig. 3. Nonetheless, it is clarified that such simplifications result in a non-negligible loss of control over the electromagnetic propagation compared to actual metasurfaces, such as the inability to achieve steep angles in steering, narrow-band operation, and ripples in reflection patterns that give rise to deep fading phenomena in cascading reflection setups, which are not limitations of metasurfaces in general [2]. Therefore, RIS-based abstractions should be understood as intentional reductions of the available wave control capabilities, rather than as physically equivalent realizations of metasurfaces. This is also reflected in their most prominent application orientation, summarized in Fig. 3.

Certain studies, particularly on RIS, have also introduced a system control models that are intended mainly for theoretical analysis. In particular, while seeking the performance bounds of a RIS unit, studies consider an optimization problem where, e.g., the SNR maximization is the driving objective and every

single phase shifter of every RIS is an optimization variable [13], [14]. Given that a single RIS can have thousands of phase shifters, it becomes apparent that this control approach is not intended for practical application. In contrast, real time control of multiple metasurfaces seeks to optimize macroscopic system level variables, such as reflection and scattering directions, the distribution of power among outgoing waves, and absorption behavior. The states of the embedded switches that, for example, manifest the steering from a direction of arrival to a reflection direction, are drawn from a database-known as *codebook*—populated during the manufacturing of a metasurface, as shown in Fig. 2.

Actual metasurfaces have had exciting applications initially in the optical regime, such as micro-lenses [15] and programmable optical scatterers [16], which led to applications in fields such as optics, spectroscopy, and high-resolution, compact imaging [17]. In addition to their optical applications, metasurfaces also exhibit promising properties in controlling electromagnetic fields [18]. For example, metasurfaces can be designed to absorb or scatter electromagnetic radiation, making them suitable for applications such as radiative cooling and electromagnetic shielding. Furthermore, metasurfaces have been used to enhance the efficiency of solar cells by manipulating the interaction between incident light and the photovoltaic material.

In the following, we focus on applications to wireless communications as the driving scenario of the tutorial. The same modus operandi, however, remains applicable for other cases, such as RF imaging. Moreover, we will assume actual metasurfaces, i.e., without loss of modeling generality. It is noted that the inductive current manipulator model encompasses the phased array derivations of Fig. 3 and, as such, the following remains applicable in their case.

B. Manufacturing Approaches for Electromagnetic Metasurfaces

Electromagnetic metasurfaces constitute the focus of the present paper, as they have recently received the research and industrial spotlight in the context of 6G integrated sensing and communications [19]. Their fabrication poses significant challenges due to the need for precise control over the periodic structure’s geometry, material properties, and interconnects. In the following, we survey some of the most significant manufacturing approaches from two aspects:

- 1) The physical aspect, encompassing the passive materials (e.g., plain metal parts) and active parts that are involved in the electromagnetic response of a metasurface. In the following, we will describe the active parts as dynamic impedance-shifting components, which constitute a generalization over phase-shifters, thus covering both metasurfaces and antenna arrays.
- 2) The logic control aspect, involving the logic circuitry required for the interaction between a computer and the metasurface, in order to modify its electromagnetic response and overall behavior. This aspect determines how metasurfaces can be integrated into software controlled networks and how rapidly and reliably configuration decisions can be enforced.

The physical aspect. This aspect comprises all parts of the metasurface that allow impinging waves to form inductive currents within or over them, as well as materials that provide structure integrity and electromagnetic isolation. Corresponding examples include copper patches, PIN diodes, dielectric substrates and prepreg materials [20]. Major manufacturing approaches and options are the following:

Lithography and Etching. Lithography and etching techniques are widely used for fabricating electromagnetic metasurfaces [21]. These methods involve pattern transfer onto a substrate using photoresist materials, followed by etching or removal of material to create the desired microstructure. The resulting structures can be used to create periodic arrays with precise control over geometry and material properties.

Nanoimprint lithography (NIL) is another approach that has been explored for fabricating electromagnetic metasurfaces [22]. This method involves creating a master structure with nano-scale features, which are then transferred onto a substrate using NIL in a stamping manner. The resulting structures can be used to create periodic arrays with enhanced electromagnetic properties.

3D Printing. Three-dimensional printing (3DP) has also been explored for the fabrication of electromagnetic metasurfaces [23]. This approach involves creating a 3D structure with nested layers of material that are precisely controlled in terms of geometry, density, and composition. The resulting structures can be used to create complex periodic patterns that exhibit enhanced electromagnetic properties, while from a system perspective, such flexibility allows the exploration of non conventional metasurface geometries, potentially enabling novel control functions.

The following commonly come as packaged electronic components, that are employed as tunability agents within the metasurface. However, as they constitute parts that allow the flow of EM inductive currents, they are studied as part of the physical aspect of a metasurface.

Varactor-based Impedance Shifters. Varactor diodes are widely used for impedance shifting due to their simplicity and tunability [24]. By varying the capacitance of the varactor, it is possible to achieve a controlled impedance shift between incoming and outgoing waves.

MEMS are employed in some impedance shifting applications due to their high precision and low power consumption [25]. By physically altering the path length of the wave, MEMS can achieve precise control over impedance shift. This technique is commonly found in advanced applications requiring high performance.

Liquid crystals are another option for impedance shifting, particularly useful for tunability across a wide frequency range [26]. The refractive index of liquid crystals can be controlled by an electric field, enabling rapid phase modulation. This technique offers flexibility and precision in metasurface design.

Graphene-based impedance Shifters. Graphene's electrical tunability makes it a promising material for impedance shifting [27]. By controlling the voltage bias, graphene's properties can be altered to achieve desired impedance shifts. Graphene-

based impedance shifters are an area of active research due to their remarkable electronic properties.

Ferroelectric impedance Shifters. Materials with ferroelectric properties are utilized for impedance modulation due to their high-speed switching capabilities [28]. Ferroelectric impedance shifters offer rapid and efficient control over impedance shift, making them suitable for applications requiring fast response times.

Mechanically Reconfigurable impedance Shifters. Mechanical changes can be used to alter the impedance configuration in metasurfaces [29]. While this technique is simpler than others, it is useful for slower-adapting application scenarios. Mechanically reconfigurable impedance shifters offer flexibility and low power consumption, making them suitable for specific use cases.

A qualitative comparative of these options are given in Table II. In terms of efficiency, high degree of control over the current flow is typically observed in impedance shifters that utilize precise impedance control mechanisms, such as MEMS, graphene, ferroelectric, metamaterial-based, and photonic solutions. These technologies enable the achievement of high-quality impedance shifting with minimal losses, making them suitable for a wide range of applications. In terms of bandwidth, MEMS and liquid crystal-based impedance shifters exhibit very wide bandwidth, which is essential for advanced applications that require precise control over the impedance-shifted signal. This high bandwidth enables these solutions to operate effectively in environments where, e.g., rapid phase modulation is necessary. The manufacturing cost of these options varies widely depending on the technology employed. Graphene and photonic shifters are generally more expensive due to the advanced materials and processing techniques required, while simpler solutions such as varactor and mechanically reconfigurable types are less costly.

In terms of energy consumption, low consumption is a primary objective for impedance shifters, as it is essential for their deployment in practical applications. Most impedance shifter solutions aim to minimize energy consumption while maintaining high performance. MEMS and graphene-based solutions are particularly noteworthy in this regard, as they exhibit low power requirements that make them well-suited for efficient operation. However, electronic impedance shifters usually require power supply to maintain a certain impedance shift state. MEMS-based and mechanical shifters may have: i) lower tuning speed, and ii) higher initial state shift consumption than their electronics counterparts, but are *state-preserving*, i.e., they do not require any power to maintain their set state. Thus, their energy consumption is marked as minimal in Table II. Notice that this depends on the impedance shifting frequency, since in fast shifting cases, the overall consumption may be defined mainly by the initial state shift energy expenditure. In other words, this distinction becomes important when metasurface reconfiguration is performed frequently or under strict energy budgets.

On assembly prospects: It is important to note that each of the aforementioned types of impedance shifters may require different assembly approaches. Since Printed Circuit Board (PCB) processes are usually more accessible to early research

Table II: Comparison of Impedance Shifter Types.

Impedance Shifter Type	Efficiency	Bandwidth	Manufacturing Cost	Energy Consumption
Varactor-based	Moderate	Moderate	Low	Low
MEMS-based	High	Wide	Moderate to High	Minimal (state-preserving)
Liquid Crystal	Moderate	Wide	Moderate	Low to Moderate
Graphene-based	High	Potentially Wide	High	Low
Ferroelectric	High	Moderate to Wide	Moderate	Low to Moderate
Mechanically Reconfigurable	Moderate	Moderate	Low	Minimal (state-preserving)

prototyping efforts [30], a possible misconception is that metasurfaces are required to come in PCB form. However, as large-scale industrial and real-work deployments draw closer, other assembly processes become more fitting. In particular, Large Area Electronics (LAE) systems involve the direct fabrication of functional electronics on expansive substrates, such as flexible or three-dimensional materials, through innovative manufacturing techniques like inkjet printing, screen printing, and evaporative deposition [31]. This approach enables seamless integration of electronic components into everyday items such as smart clothing, autonomous vehicles, and intelligent structures, unlike conventional PCB assemblies that are typically confined to flat, solid substrates with form-factor and overall size limitations. By employing innovative fabrication methods such as hybrid CMOS/LAE architectures and programmable micro-assemblies, LAE systems have become known for their design flexibility, functionality and scalability [32]. In contrast to traditional surface mount technology (SMT)/through-hole technology (THT) PCB assembly processes, which are limited by their reliance on conventional materials and manufacturing techniques, LAE enables in-situ integration of advanced materials and components, making them excellent candidates for massive metasurface manufacturing and deployment [20].

The logic control aspect. The control logic circuitry of metasurfaces enables the scalable and precise manipulation of electromagnetic waves based on external software commands, effectively forming the interface between network level control decisions and the realization of electromagnetic functionalities. The choice of logic control circuitry depends on the specific requirements of the application, including the need for flexibility, reconfigurability, and performance.

One popular approach is the use of *Field-Programmable Gate Arrays (FPGAs)*, which offer flexible and reconfigurable logic that can be easily adapted to changing needs [33]. FPGAs are well-suited for prototyping and dynamic system configuration, while commonly supporting a very large number of control pins per single package, a trait that matches well with the numerous control elements typically embedded in a metasurface. Additionally, their ability to handle complex logic operations ensures efficient processing of control signals [34].

For simpler systems, *microcontrollers* provide an efficient and cost-effective solution for managing control logic [35]. These small computers can effectively control individual elements of a metasurface, offering a straightforward approach to system management. However, as the complexity of the system increases, more advanced logic control circuitry may be required.

Application-Specific Integrated Circuits (ASICs) constitute a tailored solution in cases of specific speed, energy efficiency and/or footprint requirements [36]. Optimized for specific tasks, ASICs provide the best possible performance but come with higher development costs and limited flexibility.

Digital Signal Processors (DSPs) are an option for metasurfaces requiring advanced signal manipulation capabilities, e.g., to remodulate the inductive currents in specific ways [37]. DSPs can execute complex algorithms efficiently, enabling dynamic tunability and adaptive systems. Such processing capabilities may become relevant in cases where the metasurface behavior must occur in response to specific attributes of the incoming wave, i.e., at a complex waveform-processing level.

Another approach is to integrate both analog and digital components into *Mixed-Signal Circuits* [38], which can handle the analog nature of wave manipulation in metasurfaces while maintaining digital control for programmability. This hybrid approach enables the efficient processing of control signals while preserving the flexibility required for system integration and adaptation. In this sense, mixed signal designs offer a natural continuation of purely digital control, allowing part of the signal processing burden to be handled closer to the physical interaction with the wave.

Finally, *System-on-Chip (SoC)* solutions offer a comprehensive integration of multiple components, including processors, memory, and control logic, into a single chip [39]. SoC architectures can be designed to include specialized modules for metasurface control, providing both high performance and integration. By leveraging these advanced logic control circuitry options, researchers and engineers can develop efficient and adaptable metasurfaces that optimize electromagnetic wave manipulation for a wide range of applications. This increasing degree of integration becomes particularly relevant as metasurfaces scale in size and complexity, since it directly affects footprint, reliability, and deployment practicality.

The choice of the logic control also affects the wiring within the metasurface, which usually comes in the form of patterned metallic traces. For instance, FPGAs can support many physical pinouts, each directly controlling an active element. Moreover, they can implement assistive tasks, such as logic control break-out, by implementing impedance shifters and in some cases DC voltage regulators. It is also expected that a specifically programmed FPGA also provided very low control latency.

Employing simple microprocessors instead of FPGAs, has the benefit of lower cost and easier development, but can require external assistive circuitry that must be placed upon the

Table III: Logic Control Circuitry Options for Metasurfaces

Aspect	FPGAs	Microcontrollers	ASICs	DSPs	Mixed-Signal Circuits	SoC Solutions
Flexibility	High	Moderate	Low	Moderate	Moderate	High
Performance	High	Moderate	Very High	High	High	High
Power Consumption	Moderate to High	Low	Very Low	Moderate	Moderate	Low to Moderate
Development Cost	Moderate to High	Low	Very High	Moderate	High	Moderate to High
Complexity of Design	High	Low to Moderate	High	Moderate	Moderate	High
Speed of Operation	Very High	Low to Moderate	Very High	High	Moderate	High
Real-Time Processing	Excellent	Limited	Not applicable	Excellent	Limited	Excellent
Reconfigurability	Excellent	Limited	None	Limited	Limited	Good
Suitability for Prototyping	Excellent	Good	Poor	Moderate	Moderate	Good

metasurface, yielding extra footprint and wiring. Towards cost-effectiveness, meta-atoms can also be controlled via shared means, such as buses and cross-bars, reducing the wiring complexity and costs further, but usually the expense of control latency. This trade off illustrates how hardware control choices influence the temporal granularity at which metasurface configurations can be updated. Notably, there also exist theoretical proposals for metasurfaces comprising wireless cells, both for configuration and for energy harvesting [40].

III. METASURFACES AS NETWORK COMPONENTS

Having covered basic prerequisites from the physical layer of metasurfaces, we proceed to study their network-level modeling. In the following, we will seek to align with the concepts of network graphs, network routing and virtual network functions, which are basic working tools in the field of networking [41]–[43].

Remark 1. The ensuing model of metasurfaces as network components does not imply a store-and-forward operation model, given that metasurfaces cannot be aware of the data carried by impinging waves.

Instead, the following model is aligned to the pass-through network switching, which is used extensively in optical networks [44].

A. Modeling Metasurfaces as Wave Routers

As discussed, metasurfaces provide advanced electromagnetic control and high granularity capabilities for various applications like wide-band communications, energy harvesting, ultra-high resolution medical imaging, sensing, quantum optics, and military use cases [45]. They are well known for their ability to create pencil-like beams (known as collimation), non-reciprocating behavior (i.e., reflecting towards one direction with excellent efficiency, but absorbing in the reverse), as well as operating as frequency filters. Moreover, designs exist for virtually any operating band, from MHz to THz and beyond.

Metasurfaces can support multiple EM interactions including reflection, refraction, absorption, and polarization. These four interactions can be considered as basic *EM Functions*, as shown in Fig. 2. Complex functionalities can be built by combining these basic functions, as shown in Fig. 4. This combining occurs by following merging rule on the corresponding configurations of the EM Functions to be merged. For instance, a new, complex EM Function can be created by defining V_i^* as the mode $\vee_i \{V_i\}$, V_i being the bias signal value applied to the

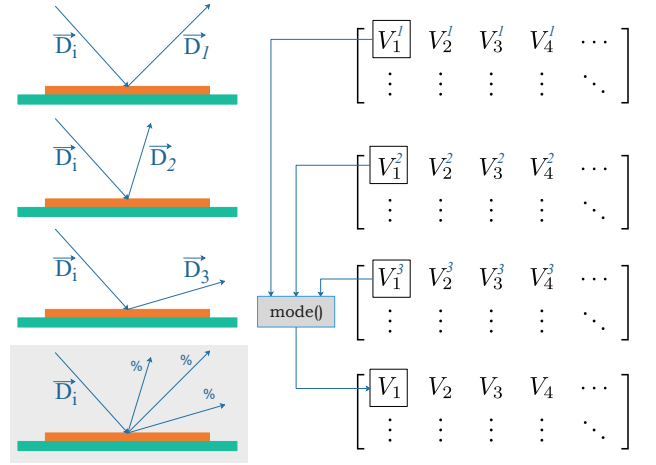


Figure 4: A process of compiling complex EM metasurface Functions from basic ones [46]. In the illustrated example, a 3-way split is compiled from three basic wave steer EM Functions. (The mode is the value that appears most often in a set of data values, following a rounding step).

i^{th} cell, as shown in Fig. 2 and 4. Naturally, merging multiple functionalities results into a lower degree of efficiency for each one, compared to the case when only a single EM Function is activated.

For instance, let f_1 denote a specific EM Function performing, e.g., steering of waves incoming from a direction \vec{i}_1 , towards a direction \vec{o}_2 . Let e_1^i be the total power impinging upon the corresponding metasurface from the intended direction \vec{i}_1 , and e_1^o be the total power that the metasurface manages to reflect towards \vec{o}_2 . The efficiency ϵ_1 of f_1 is defined as [47]:

$$\epsilon_1 = \frac{e_1^i}{e_1^o}. \quad (1)$$

Proceeding, consider a second EM Function, f_2 , which can freely perform a different type of steering, direction-dependent absorption, etc. Let ϵ_2 be its efficiency when being deployed alone in the same metasurface. Now let's consider that both f_1 and f_2 are deployed together in the metasurface by following the mode rule mentioned above.

Remark 2. The mode rule yields a new combined functionality performing both tasks at the same time. However, when measured separately, the updated efficiency of each function will be:

$$\epsilon'_1 \leq \epsilon_1 \text{ and } \epsilon'_2 \leq \epsilon_2, \quad (2)$$

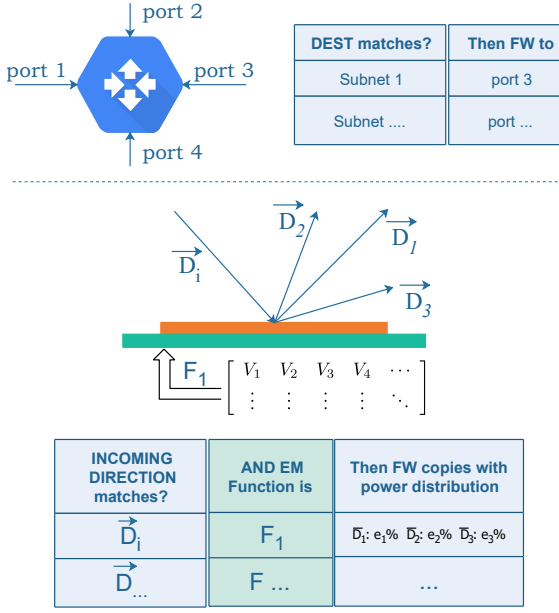


Figure 5: Visualization of the router model for metasurfaces. Top: the classic, destination-based routing process found in wired networks, following a port forwarding table. Bottom: an equivalent table form, describing the incoming wave redirection achieved by a metasurface. The redirection outcome depends on the incoming direction and the activated EM Function.

i.e., the efficiency of each function will be reduced. The equality in relation (2) holds on special cases where two or more EM functions can be served with the same $\{V_i\}$ values.

Notice that one can freely combine any number of function minding, however, the associated efficiency drop. Further details on this topic can be found in the related literature, covering the cases of how to combine multiple EM functions to attain some specific efficiency degrees, and how to price them using a resource sharing paradigm [47].

The described concept of EM Functions can be leveraged when configuring a single or a set of metasurfaces to serve the objective of user(s), which cannot consider the direct optimization of the active elements due to practical reasons. A single metasurface can have thousands of active elements, each with a multitude of possible values. Thus, treating them as direct optimization variables is impractical, especially for real-time operation.

Instead, metasurfaces can be modeled in terms of macroscopic inputs and outputs, i.e., directions of arrival and departure expressed via the concept of EM Functions. Optimizing the behavior of a metasurface then corresponds to an objective of connecting input directions to output directions, which has the benefits of:

- Reducing the dimensionality of the problem, compared to the direct optimization of impedance shifts.
- Allowing for a model akin to that of routers in classic

wired networks [8], which is very well-known in the networking field, and comes with a framework for ensuring connectivity, following graph path-finding approaches.

Thus, the proposed model integrates a forwarding table into each metasurface, which is analogous to the concept of forwarding tables found in computer networks, and is visualized in Fig. 5. This integration serves several purposes:

- *Treat wave directions as discrete input/output ports via Column 1.* In essence, not every possible direction vector is practically useful for the operation of the system as a whole. A metasurface seeks to reflectively connect users and metasurfaces, i.e., form metasurface-metasurface, user-metasurface or user-user reflections. From these discrete targets, metasurfaces have fixed relative points in space, while the position of users can also be discretized.
- *Describe the metasurface behavior under different EM functions via Column 2.* This entry also lists the supported EM functions, i.e., configurations that have been tested and profiled during the manufacturing stage.
- *Describe the scattering radiation as a “leaky multicast” action via Column 3.* This entry includes profiling measurements pertaining to an EM Function identifier and an incoming wave direction. Following the aforementioned profiling process by the manufacturer, it consists of a hash map connecting output directions/ports to the associated power loss measured exactly when departing the metasurface. Thus, the scattering phenomenon becomes akin to packet multicasting, albeit with the extra attribute of associated power loss. (A path loss rule can yield the total power losses at a distance along an output port).

Thus, by combining a forwarding table functionality with EM Function support and profiling measurements, the proposed router model for metasurfaces offers a connection to existing framework for managing and configuring complex networks, even in real-time.

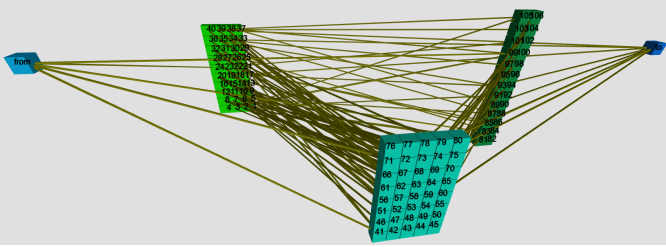
Remark 3. The routing table may not be stored as an exhaustive list of entries. In general, it is a service that produces a resulting power distribution, given an incoming direction of a selected EM Function.

In the following, we leverage the router model to treat a complete metasurface-enabled wireless system as a graph, and formulate configuration objectives as path finding problems.

B. Describing Systems of Metasurfaces

In everyday communication scenarios, multiple wireless users often interact within physical spaces. In such environments, electromagnetic waves freely dissipate, leading to interference and potential eavesdropping among devices.

In contrast, the concept of PWEs employs metasurface coatings placed on walls and ceilings in the form of tile-like units, in order: i) to describe systems of metasurfaces, and ii) offer user-defined wireless propagation [1]. PWEs receive software commands from network administrators and adapt their interaction with electromagnetic waves to meet user needs. For instance, Figure 7 (top) demonstrates a situation where a user requires enhanced security against eavesdropping. The



wave undertook in order to eventually reach the receiver. Each point is marked by an arrival delay (τ_k) measured from the time the signal was transmitted, and a received power level (P_k). In essence, the PDP describes how the received copies of the original signal (due to reflection, refraction, etc.) get distributed over time and power, providing insight into the channel's characteristics and behavior. Understanding the PDP is crucial in wireless communication systems, as it informs the design of transmission strategies, modulation schemes, while defining the achievable data transfer rates.

PWEs can craft the PDP per user pair by routing a signal via the PWE graph and over specific paths with known delay, and potentially predictable power loss [8]. This engineered PDP could lead to the mitigation of multipath fading phenomena. Alternatively, a "multipath amplifier" effect can be enforced when signal obfuscation is required instead. PWEs can create multiple simultaneous signals with destructively superposing arrival times and amplitudes, simulating complex multi-path environments. In general, by precisely controlling the wave routing process, PWEs can engineer the PDP of the wireless channel to test various transmission strategies, modulation schemes.

While the PDP optimization constitutes an overarching goal, it is possible to define simpler metrics based on it, in order to facilitate the optimization computations. One such approach is to define a simple scalar metric over the PDP data. One such metric, commonly used in wireless communications, is the Root Mean Squared-Delay Spread (RMS-DS), defined as [49]:

$$R_\sigma = \sqrt{\bar{\tau}^2 - (\bar{\tau})^2} \quad (3)$$

where

$$\bar{\tau} = \frac{\sum_{\forall k} P_k \cdot D_k}{\sum_{\forall k} P_k} \text{ and } \bar{\tau}^2 = \frac{\sum_{\forall k} P_k \cdot D_k^2}{\sum_{\forall k} P_k}. \quad (4)$$

A channel model with low R_σ corresponds to a multipath setting where the PDP is closer to equalization, i.e., minimal fading effects. However, a deceptively minimal R_σ value can also stem from keeping just one path out of the $\{P_k, \tau_k\}$ set, while the rest are driven away from the receiver, hence reducing the overall received power.

Thus, defining PWE optimization metrics over the PDP typically needs to consider accompanying conditions that should be upheld from a PWE configuration solution.

A. An Optimization Framework for PWEs

Consider a PWE with a set of users $u \in U$, and a set of performance metrics, \mathbf{M} , from which each user can select a subset $M_u \subseteq \mathbf{M}$, iterated as $\mu_u \in M_u$, in order to define his requirements from the PWE. Examples can include the maximization of his signal-to-interference-plus-noise ratio, the maximization of power harvesting rate, latency minimization, the minimization of the signal exposed to other users, etc.

The PWE is composed of a set of tiles N , and a set of EM functions, \mathbf{F} , from which each tile $n \in N$ supports a certain subset $F_n \subseteq \mathbf{F}$, iterated as $f_n \in F_n$, due to manufacturing diversity or placement properties. Examples include PWEs with mixed metasurface and RIS units, and tiles placed in

open spaces versus under severe blockage with corresponding wave steering diversity potential, respectively. The set \mathbf{F} is considered to contain all possible merged functionalities as well (described in the context of Fig. 4). Deactivation of tile n (i.e., yielding regular, non-metamaterial behavior) will be denoted as $f_n = \emptyset$.

Furthermore, we define the following comparator:

$$c(f, f^*) = \begin{cases} 1 & \text{iff } f = f^* \\ 0 & \text{iff } f \neq f^* \end{cases}. \quad (5)$$

PWEs need to be re-configured in order to adapt to changing user requirements, user mobility or time-variant blockage in the environment. Consider a notation describing the optimal PWE configuration at a round $t-1$, and at round t as $f_n^{t-1}, \forall n$ and $f_n^t, \forall n$, respectively. Then, the number of updates required to migrate from f_n^{t-1} to f_n^t is:

$$R^t = \sum_{\forall n} (1 - c(f_n^{t-1}, f_n^t)) = \|N\| - \sum_{\forall n} c(f_n^{t-1}, f_n^t) \quad (6)$$

Notably, one should keep the number of updates minimal, throughout the operation rounds of a PWE. In other words, follow a proactive policy that ensures that no major increase should occur in R^t , as this can correspond to extensive changes in the PWE configuration, increasing control latency and potentially leading to unintended behavior (as shown later, in Fig. 10). Moreover, the number of unused (free) tiles at round t is:

$$S_\emptyset^t = \sum_{\forall n} c(f_n^t, \emptyset) \quad (7)$$

In general, one should keep S_\emptyset^t maximal at every t , in order to both increase the service capacity of the PWE (i.e., be ready to accommodate changes in the next round), and to be economic in terms of energy consumption and administrative overhead. However, keeping R^t minimal through the operation rounds is a more pronounced concern over S_\emptyset^t .

We proceed to formulate the general optimization objective of a PWE at time t as follows:

$$\begin{array}{ll} \text{opt:} & \{f_n^t \in F_n, \forall n\} \{ \mu_u^t \in M_u, \forall u \} \\ \text{min-max:} & R^t, \forall t \\ \text{max:} & S_\emptyset^t \end{array}, \quad (8)$$

where:

- 1) the first line expresses the selection of tile functions for the fulfillment of user requirements are first priority,
- 2) the second line expresses the constraint over successive PWE updates, and
- 3) the third line the maximization of free tiles in the system only at round t , denoting it as last priority.

Notice that the formulation (8) considers the transmission and receptions characteristics of the users to be predefined. In other words, parameters such as the transmission power and user antenna directivity are considered to be set. This can be generalized by considering the user devices that also support a corresponding set of special EM Functions (slightly abusing the term definition to cover user devices apart from tiles), where an optimal choice must also be made.

In the general formulation (8), a solution $\{f_n^t \in F_n, \forall n\}$ is assumed to be Pareto-dominant across all three aforementioned concerns. This approach on itself can be restrictive, as a valid solution may potentially not be possible. Thus, more relaxed expressions can be obtained such as by employing pre-defined limits R^{max} and S_\emptyset^{min} such that:

$$\begin{aligned} \text{opt: } & \{f_n^t \in F_n, \forall n\} \{ \mu_u^t \in M_u, \forall u \} \\ \text{subject to: } & R^t \leq R^{max} \\ & S_\emptyset^t \geq S_\emptyset^{min} \end{aligned}, \quad (9)$$

where the latter two conditions should be treated as weak. Other simplifications would be to incorporate the three clauses of formulation (8) into one sum using weights, as per the standard practice for simplifying Pareto-dominant formulations. We proceed to make the following further remarks regarding:

- the consistency of the updates, and
- the complexity

of either formulation. Regarding the update consistency:

Remark 6. Consider a current PWE configuration, $\{f_n^t \in F_n, \forall n\}$, and a planned one, $\{f_n^{t+1} \in F_n, \forall n\}$, set to be deployed at $t + 1$. The update schedule, i.e., the order of with which each tile t will migrate from f_n^t to f_n^{t+1} requires consideration of transient effects.

For instance, consider that the first tile near a transmitter, n_1 , migrates to $f_{n_1}^{t+1}$ before all other tiles. The subsequent propagation would be unintended, potentially yielding interference, attenuation and eavesdropping potential. We denote this problem as update consistency and study it in the ensuing section IV-B.

Regarding the complexity:

Remark 7. A performance metric μ_u can be strongly dependent to a small subset of $\{f_n\}$ and independent to the rest.

We consider the following supporting example. Let a PWE configuration $\{f_n\}$ leading to a metric μ_u for user u , expressing his received power of the useful signal. The function $\mu_u(\{f_n\})$ is strongly influenced by only a subset of the total set of configured tiles which form a cascading path by steering power from one to another. Changing any of these functions completely (e.g., set to absorb, or steer somewhere off-path) will result to a sharp reduction of μ_u . On the other hand, changing the EM Function of any tile in the PWE, which does not receive impinging waves destined to u , will have no effect on μ_u .

Remark 8. A performance metric μ_u can be highly discontinuous with regard to its strongly dependent tile functions.

The rationale follows the previous example, i.e., abrupt steering changes at tile over a path lead to sharp decreases in the μ_u values, hence discontinuities in $\mu_u(\{f_n\})$. However, altering a tile function to, e.g., yield a slightly different efficiency degree ϵ , as defined in relation (1), leads to slight μ_u value changes and, hence, defines a relatively small, continuous region of $\mu_u(\{f_n\})$.

These remarks support that solving the PWE configuration optimization problem requires knowledge of the PWE graphs properties. (Here we exclude simple cases that can be solved via exhaustive search, i.e., those with very few tile-, user-, and

EM function-combinations). We make note of some interesting such relations later, in Section VIII-A which outlines the related open challenges.

B. Consistent Update Formulation

In this section, we formalize the problem from a consistent network update perspective. The formalization of this section ensures that path updates discussed in the next section (Section IV-C) are realized as they are envisioned, considering possible delays in updates applied in each tile. In doing so, we provide a tutorial on building a mixed integer linear program, which ensures consistent network update, while minimizing the number of rounds, or the number of updated tiles, as discussed in the previous section (Section IV-A).

We first point out that the problem at hand closely ties with the similar problem that exists in the context of *software defined networks (SDNs)*. An SDN-based network design allows for a centralized software program, to take the control of multiple data-plane elements, allowing for a more flexible and efficient traffic engineering [50]. However, such a centralized control comes with its own challenges, in particular in terms of consistency of network updates: due to the inherent differences between networking elements, they might perform updates out of the intended order by the centralized control, which might result into the formation of transient networking loops or black holes [51], [52]. As mentioned earlier, such issues, in the context of PWE can result in multipath reverberation or total signal loss. A suggested solution to keep updates consistent is to perform updates in rounds, in such a way that any possible order of updates in a round does not result in one of the aforementioned problems [53].

Another optimization objective that has been studied in the context of SDNs, and closely ties with the optimization of parameter R^t , is the number of switch interactions (touches) [54]. Number of touches, in the context of PWEs, can be translated to the number of tile interactions, which formed the basis of our formulation.

In the following formulation, we provide an exact Mixed Integer Linear Program (MILP) formalization, to minimize the total number of interactions with RIS units (touches), considering certain number of rounds (rounds). This formulation utilizes the following variables:

- For a tile u , we consider the binary variable a_v^t to indicate tile u being active at round t . Additionally, for such a tile, we consider an integer variable o_u^t , which indicates an order for tile u at round t .
- For a link (u, v) (there exists a link (u, v) if tiles u and v have a LOS or nLOS), and round t , we define an activity variable $a^t(u, v)$, which is one if both u and v participated in a communication path at round t .
- For a pair of tiles u, v , we define the integer variable $dis_{u,v}^t$ to denote distance between u and v at round t . Furthermore, considering another tile w , we consider an auxiliary binary variable $a_{u,v,w}$.

For all the variables above, the (s, d) in the superscript of variables indicates that the variable is for transmitter s and receiver d . Furthermore, we assume that at the round t , we

Algorithm 1 Consistent Update Formulation

```

1: Minimize touches
2:  $\sum_{t=1}^{\text{rounds}} \sum_{u=1}^n c(a_u^t, a_u^{t-1}) \leq \text{touches}$ 
3: for all  $t < T$  do
4:   for all  $(u, v) \in E$  do
5:      $a_{(u,v)}^t \leq a_u^t, a_{(u,v)}^t \leq a_v^t$ 
6:      $a_{(u,v)}^t \leq \text{dis}_{u,v}^t$ 
7:      $a_{(u,v)}^{t,(s,d)} \leq a_{(u,v)}^t \quad \forall (s, d)^t \in P^t$ 
8:   end for
9:   for all  $\forall u, v, w \in V$  do
10:     $\text{dis}_{u,v}^t \leq \text{dis}_{u,w}^t + \text{dis}_{w,v}^t$ 
11:     $\text{dis}_{u,v}^t \geq \text{dis}_{u,w}^t + \text{dis}_{w,v}^t - M \cdot (1 - a_{u,v,w})$ 
12:   end for
13:   for all  $(s, d)^t \in P^t$  do
14:      $\sum_{\forall (s,v) \in E} a_{(s,v)}^{t,(s,d)} = 1$ 
15:      $\sum_{\forall (u,d) \in E} a_{(u,d)}^{t,(s,d)} = 1$ 
16:      $\sum_{\forall (v,w) \in E} a_{(v,w)}^{t,(s,d)} = \sum_{\forall (w,u) \in E} a_{(w,u)}^{t,(s,d)}, \forall w \in V \setminus \{s, d\}$ 
17:   end for
18:    $a_{(u,v)}^t + \frac{o_u - o_v}{|V|-1} \leq 1 \quad \forall (u, v) \in E$ 
19: end for

```

have access to the list of transmitter-receiver pairs as P^t . In this formulation, we consider M to be a very large integer (at least larger than the number of tiles).

The overall design of Algorithm 1 is as follows. It first ensures that the number of tile changes is capped by R . Here, we use the comparator c defined in equation (5). We then ensure that the paths between a transmitter and receiver are the shortest paths, and keep track of tiles that need to be active in each path. In this formulation, we use a variant of Miller-Tucker-Zemlin formulation [55] to ensure loop-freedom during the update.

In order to speed up our MILP, in case a near-optimal result would be sufficient, we can use a *linear program relaxation*, and then get an exact update order of tile updates through (randomized) rounding.

C. Approximations based on Heuristics and Path finding Algorithms

In the preceding Sections, it was shown that a formal PWE optimization can be computationally intensive. Therefore, approximate but efficient heuristics has been proposed in the literature and are surveyed below.

1) *Path Finding-driven Approximations*: Consider a set of users in a PWE graph. Let the tiles in the LOS vicinity of each user be denoted as *first-contact* tiles. The path-finding approach involves finding routes that connect the first-contact tiles of user 1, to the first contact tiles of user 2. This can also be generalized for multiple users.

A straightforward approach is to model this objective as a k-shortest paths problem [56], using the link loss (derived by the link distance and any consequences of Remark 5) as the cost metric. The intuition behind this method is that by utilizing multiple paths, the received signal power can be accumulated,

while minimizing delay helps reduce delay spread and power loss, especially in environments with abundant path diversity. This approach can be extended by incorporating a more sophisticated cost function that captures additional performance factors.

Although traditional k-shortest or similar path algorithms can be applied, they must be adapted to enforce certain constraints that may be set. Major factors include:

- Using only up to a specific number of EM functions per metasurface simultaneously, which puts a limit to the number of air routes that can intersect at any given graph vertex.
- A user set prioritization policy, such as finding paths for the most distant user pairs first [8], since initial path finding attempts are likely to yield better results, compared to when parts of the graph have been already marked as occupied by EM functions.
- Filtering the possible paths further, e.g., by avoiding links near possible eavesdroppers, or by requesting that the final link be perpendicular to the mobility trajectory of the receiver, in order to mitigate Doppler effects in mmWave communications. (An example is evaluated later, in Section VII).

Furthermore, while the k-shortest paths formulation offers a reasonable starting point, more advanced formulations are needed to fully capture the multi-objective nature of the problem. For instance, one can adopt a multi-objective optimization framework that treats delay and signal strength as separate objectives. This allows for a more nuanced exploration of the trade-off between these often-conflicting goals. Achieving this requires more sophisticated algorithms capable of handling multiple objectives such as multi-objective heuristic optimizers, Pareto optimization methods, or scalarization techniques like the weighted sum approach. The latter can reduce the multi-objective problem to a single-objective shortest path problem by combining objectives into a single cost function.

We also note that the optimization of the number of updated tiles has close ties with the problem of *lexicographical shortest path* [57], in which the shortest path should be determined based on multiple objectives. The algorithms for this problem are an extension of shortest path algorithms that use the *best-first search* approach [58] (similar to the Dijkstra algorithm). In the context of our problem, we briefly describe a greedy algorithm that works as follows: Initially, it sorts transmitter-receiver pairs based on their preserved distances, in an ascending manner. It also initializes a set to keep track of tiles that have been part of the shortest path. Then, for each transmitter-receiver pair, we build the shortest path as follows: we run a Dijkstra algorithm, with the difference that in each step, if two tiles have the same distance, we select the one that has already been part of the shortest path before.

2) *Propagating Heuristic-driven Approximations*: Propagating heuristics are a vast class of approximate solvers, which rely on the progressive exploration of a solution space [59]. They can be categorized as back-propagating or front-propagating, depending on their direction of operation. Front-propagating initiate from a known initial state and attempt to reach an optimal one, while back-propagating

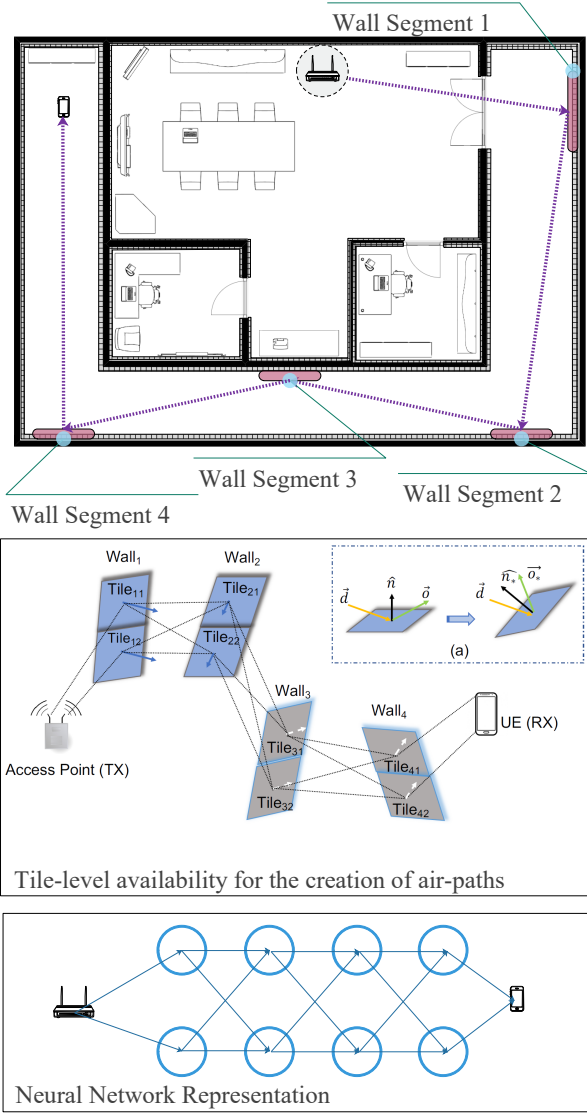


Figure 7: Overview of a back-propagating heuristic for PWE optimization. Top inset: an exemplary floorplan where the walls are covered with metasurface tiles. Middle inset: A selection of wall segments is made, which will connect two wireless devices via wave propagation engineering. Bottom inset: a corresponding neural network is constructed, which seeks to attain a required level of performance at the receiving end. Inset (a): once the back-propagation process is complete, each neuron is mapped to an EM Function depending on the similarity between the neuron's weights and the EM scattering profiles that can be attained by the corresponding metasurface.

heuristics start from the required, optimal conditions and attempt to find initial states that correspond to them. In the following, we provide a brief tutorial on their application to the problem of PWE optimization.

a) Back-Propagating: This direction is expressed via the concept of using neural networks to optimize wireless communication systems by making the architecture directly

interpretable [60]. Each neuron in the network corresponds to a specific part of the system being modeled, providing a direct correspondence with how the network processes information. The state of a neuron directly reflects the EM Function of a metasurface tile, allowing for an automated mapping of the state of a trained neuron to an EM Function that should be enabled. The concept is visualized in Fig. 7.

The number of layers and nodes in each layer is determined by the number of walls with metasurface tile coating that a transmitted wave will impinge upon before reaching its intended receiver. In other words, a rough per-wall routing decision is made first, using classic algorithms such as Dijkstra or A* [59], [61]. (Notice that this employs a different graph than the one described in section III-C). This approach ensures that the network captures the general layout of the physical environment. The input layer represents the initial conditions at the transmitter side, while the output layer represents the required, optimal conditions expected at the receiver side.

A multi-layer perceptron neural network is employed because it enforces similar activation and actuation of its neurons, aligning with how tiles manipulate the flow of electromagnetic waves from a transmitter to a receiver. Back-propagation is used to adjust the nodes based on the received power pattern at the output layer in the previous feedforward step. A linear ramp is used as the node activation function to align with energy conservation principles of wireless propagation.

b) Front-propagating heuristics: Forward propagating heuristics assume a set of solution space-exploring processes, which can either be centrally coordinated or distributed in their workflow. Initially, each searcher explores in random directions. When one searcher discovers a promising solution, it retraces its path back to the starting point, leaving behind heuristic information to guide future searches. This information influences other searchers to follow the same path with greater likelihood, leading to convergence on an optimal solution. This process is a form of reinforcement learning and serves as a flexible optimization framework with various applications.

In the context of PWE optimization, this established optimization process cannot be directly applied, as the optimization parameters are not the links and weights to be selected. Instead, the challenge lies in selecting the appropriate EM Function for each metasurface. This selection alters the attributes of multiple links connected to the corresponding metasurface, depending on the direction of the impinging wave. This results in a dynamic optimization problem in which the graph changes as a wave propagates through it.

To address this novel graph routing problem, a forward-propagating heuristic process can exemplify operate as illustrated in Fig. 8 [62]. The process begins with explorers being released from the transmitter and traveling along each link towards the nearest metasurface (top left panel). When an explorer reaches a free metasurface, it selects one of the available EM functions randomly, using their associated heuristic information as a probability distribution function, as shown at panels at row 1, column 2 and row 2, column 1. (This does not imply an exhaustive listing of all possible

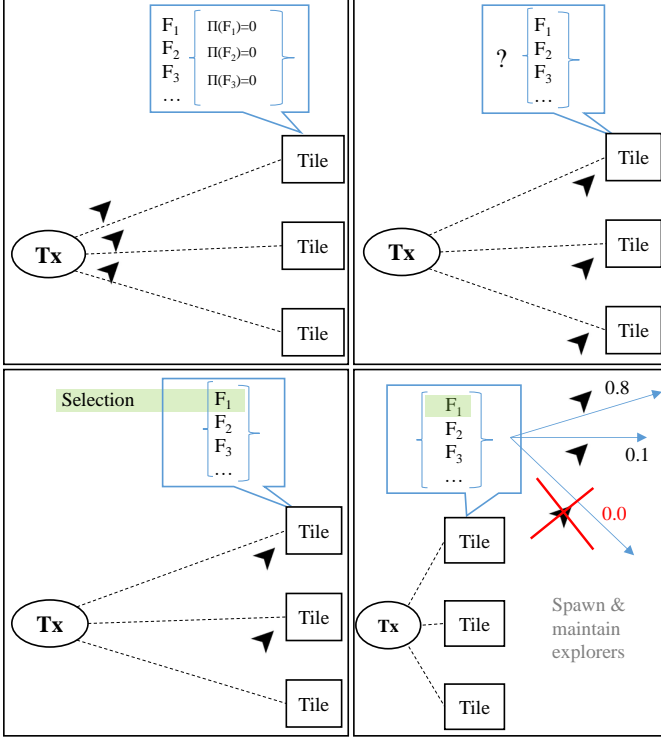


Figure 8: An example of a forward-propagating heuristic for configuring PWEs. Top left: initialization. Top right and bottom left: stochastic EM selection based on the explorers' accumulated knowledge. Bottom right: Spawning and maintaining explorers based on the EM selection at a metasurface tile.

EM functions, but just the selection of one possible EM Function). Initially, this distribution is uniform but is updated throughout the process. Once an explorer activates a function, it is destroyed but also generates a group of new explorers based on the corresponding output distribution, in order to capture the dissipating nature of EM waves. Each new explorer carries information about the cumulative propagation delay experienced so far and the remaining wave power. Notably, any explorers whose remaining wave power falls below a predetermined threshold are discarded, preventing unnecessary processing time. The process then repeats for all other explorers in the graph.

It is important to note that explorer advancement can be performed centrally in rounds (i.e., all explorers are advanced by 1 hop per round until the process concludes), or completely autonomically. Once an explorer reaches a receiver, the explored wave route is kept in a list maintaining the top- n paths in terms of power. When all explorers have concluded, a wave route selection takes place, in order to optimize the value of the selected metric. The process can accommodate multiple receivers and transmitters. In such cases, explorers carry an identifier denoting their intended receiver to distinguish between useful signals and interference.

V. THE PWE INTEGRATION TO COMMUNICATION SYSTEMS

We proceed to describe the control workflow of PWEs, and their integration to existing networks and resource allocation systems.

A. The PWE Workflow as a Networked System

The operating workflow of a PWE involves a dynamic interplay between user devices, metasurfaces, the existing network infrastructure and a central orchestration service [63]. Figure 9 outlines four major steps comprising this workflow as follows:

First, the metasurfaces are physically installed on walls, ceilings, etc., and connect to the existing local network, receiving IP addresses and advertising their availability and operating status to an orchestrating server, as shown in Fig. 9-a. (Notice that the orchestrating server is a software process, which can be hosted within existing computers, routers, or access points).

Second, and at least once after their installation, the metasurfaces are represented within the orchestrating process in the form of the aforementioned graph. This process is semi-automatic. Akin to common smart devices, the metasurfaces are registered to parts of a floorplan in a coarse manner. An extensive beam scanning and steering process follows (Fig. 9-b), with the objective of detecting line-of-sight visibility (i.e., link existence) and link characteristics (i.e., attenuation and delay) among metasurface pairs. Metasurfaces can be equipped with assistive circuitry, such as infra-red transceivers to efficiently perform this task [64]. The objective of this process is not just to derive the coordinates of the locations of metasurfaces, but rather to create a graph representation of the PWE within the orchestrator's software process.

Third, users are registered to the PWE and express their performance objectives. Users become aware of nearby PWEs through broadcast messages advertising its existence. These announcements facilitate device-to-environment association using shared authorization mechanisms. This interaction enables PWEs to recognize and accommodate the presence of user devices within their vicinity. Upon this initialization process, users state the service objectives they wish to pursue (e.g., enhanced security, wireless power transfer, quality of service).

Notably, the user initialization also involves his continuous tracking by an existing user localization system operating independently within the PWE. Exemplary approaches include optical tracking [65], or RF-driven tracking employing artificial intelligence [66]. Notably, metasurfaces exhibit inherent capabilities that enable them to function as user localization devices themselves [67]–[70].

Users in service maintain an open control channel to the orchestrator to relay updated objectives and performance metrics, and receive beamforming instructions for their devices, in order to optimally match their RF emissions to the status and location of the metasurfaces. (To manage these transitions, mechanisms adapted from Session Initiation Protocol can be

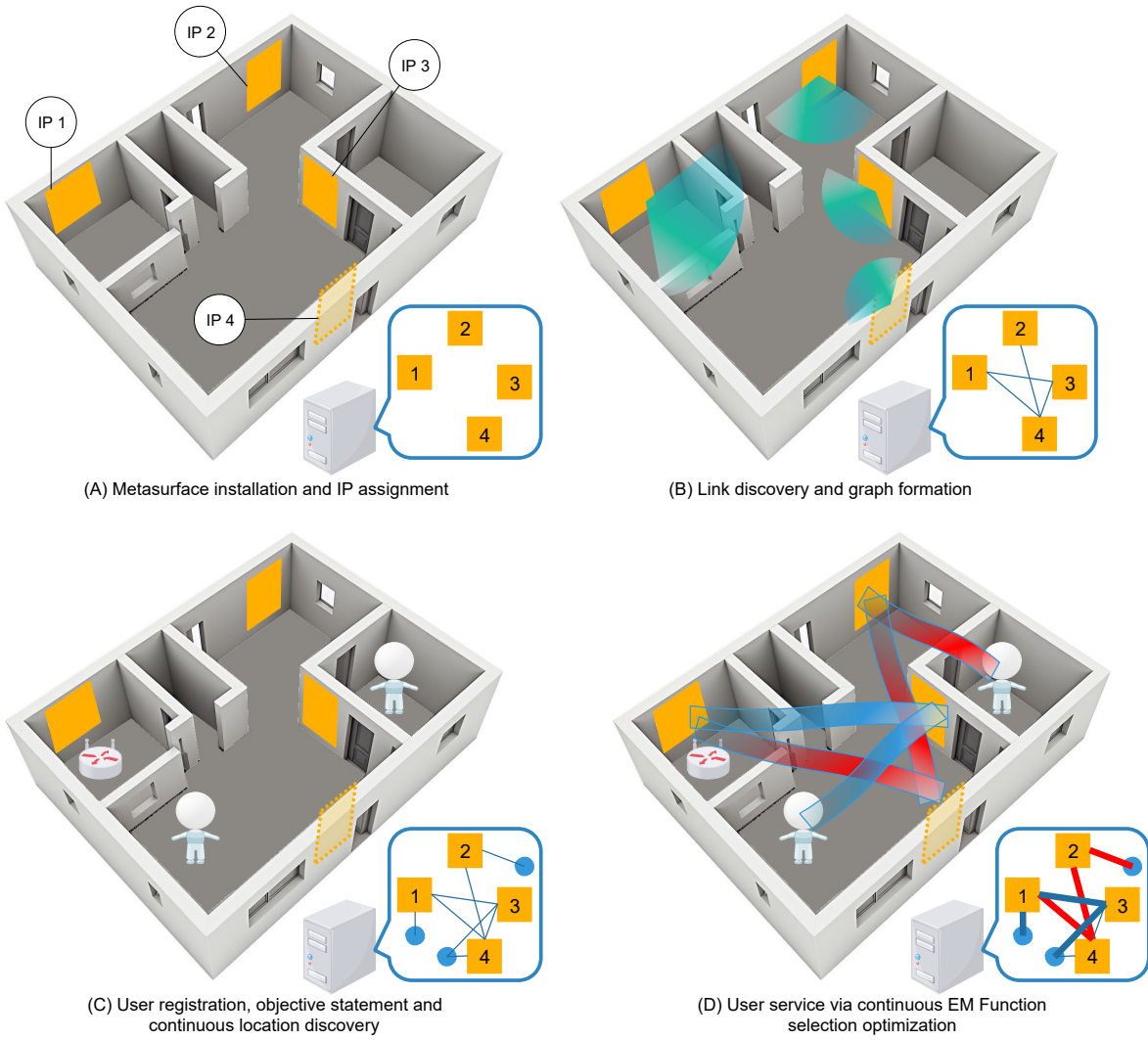


Figure 9: The four major steps of the PWE workflow: a) Metasurface units are physically installed and receive Internet Protocol (IP) addresses. b) The metasurface linkage is detected following a manual entry or automated process (beam scanning). c) Users register to a web service and state their objectives within PWE. d) The user locations are continuously tracked and the PWE is orchestrated accordingly, following a graph optimization algorithm.

employed [71], streamlining communication between devices and PWEs).

Finally, the orchestrator executes a graph optimization algorithm, as described in the previous section, and deduces the optimal EM Functions for each metasurface, matching the user objectives and positions. These EM Functions are relayed to the metasurfaces via the IP network, hence becoming *deployed*. The PWE enters a continuous cycle of receiving new user registrations, new user objectives or updated user positions and maintaining the EM Functions deployed to each metasurface.

To optimize PWE configuration effectively, the orchestrator needs to accurately detect the wavefronts emitted from user devices. This can be achieved through various methods, including the use of built-in sensors within metasurfaces or by leveraging compressed sensing principles in a sensor-less approach.

However, in mobility scenarios, as illustrated in Fig. 10, delays in completing the sense/process/configure cycle can

lead to misaligned user emissions and metasurface configurations, ultimately resulting in sub-optimal wave routing [72]. Thus, the network infrastructure and protocols involved in the communication between the orchestrator, the user localization systems and the metasurfaces is of critical importance, introducing interesting research challenges discussed later, in section VIII.

B. Interfacing with Existing Networks: A Standardization Driven Aspect

The standardization landscape for metasurfaces, mainly via their RIS variation, is rapidly evolving and involves multiple complementary organizations and forums addressing different aspects of the technology, in order to interface it with the existing network infrastructure. Three major integration directions are presently studied, each via a corresponding set of bodies:

- 1) ETSI ISG (Industry Specification Group) RIS leads the effort by defining metasurface fundamentals, archi-

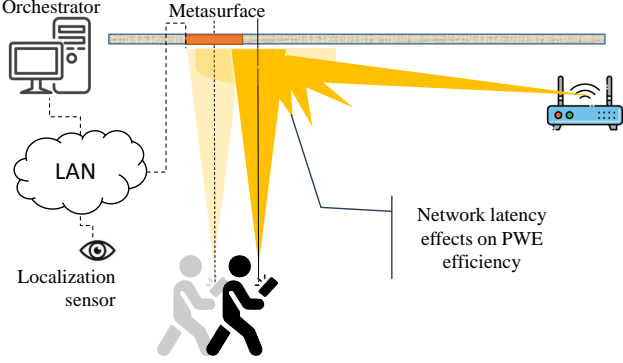


Figure 10: Overview of the PWE adaptation workflow, where a server that continuously monitors wave emissions from users and dynamically configures the metasurfaces. The performance of the network connecting the control elements of the PWE has important effects on its efficiency.

lectures, channel models, testing methodologies, and management aspects to prepare the ground for future normative standards.

- 2) ETSI ISC (Integrated Sensing and Communication) RIS consider metasurfaces within broader studies on communications evolution towards 6G, capitalizing in Integrated Sensing and Communication (ISAC) [19]. IEEE contributes through research-driven standards and publications, particularly in antennas, propagation, and measurement techniques. (In a similar but independent manner, ITU-R and 3GPP provide spectrum- and propagation-related frameworks relevant to metasurface deployment and interfacing with specific systems such as Non-Terrestrial Networks and Radio Access Networks [73]).
- 3) ETSI ISG NFV (Network Functions Virtualisation) investigates the use of metasurfaces as a cloud resource.

Together, these sets of bodies form a coordinated standards ecosystem shaping the industrialization and future integration of metasurfaces into next-generation wireless networks. We proceed to survey the technical integration focus and activities of each.

ETSI ISG RIS is an Industry Specification Group within ETSI focused on enabling programmable and controllable radio environments through metasurfaces. The group develops use cases, architectures, channel models, testing frameworks, and management concepts for RIS, targeting integration into 5G-Advanced and future 6G networks. Over a series of documents [74, ETSI GR RIS 001-008], this group has surveyed the following topics:

- Architectures, operating modes, and frequency ranges for future wireless networks along with key-use cases where metasurfaces can enhance coverage, spectral efficiency, beam management, physical-layer security, localization, sensing, and energy efficiency. Additionally, deployment scenarios across indoor, outdoor, hybrid, static, and nomadic environments are considered. Control plane options and outlines technical, interoperability, and regulatory requirements are discussed.

- Metasurface-internal architectures, control modes, hardware structures, and fabrication options, highlighting trade-offs between flexibility, complexity, and performance.

- Communication and channel models for metasurfaces, covering both near-field and far-field regimes. It defines deterministic and statistical channel models, including path-loss, multipath, interference, reradiation, and polarization effects across sub-6 GHz and high-frequency bands. Metasurface-aided device localization and sensing models, including SISO, MIMO, metasurface-aided, and metasurface-standalone scenarios. Channel estimation methodologies and key performance indicators (KPIs) for quantifying the metasurface capabilities and performance are also discussed, along with robust performance specifications.
- Explicit metasurfaces (as opposed to simple RIS) capabilities are briefly discussed, including transmission, sensing, analog computing, and caching.

In other words, the first integration consideration, studied by ISG RIS, is to provide a clear specification of the physical layer of metasurfaces, their associated performance metrics and signal processing techniques relating to wireless channel models.

ETSI ISG ISAC is an Industry Specification Group within ETSI that focuses on the joint design and integration of communication and sensing capabilities. As metasurfaces can shape, reflect, refract, or focus electromagnetic waves, enabling the network to create favorable propagation conditions for both data transmission and sensing, ISAC systems extend their sensing coverage, enable virtual line-of-sight links, and improve detection, localization, and tracking accuracy, especially in NLOS or obstructed environments. Metasurfaces act as passive or semi-passive sensing enablers, creating additional sensing paths and angles without adding active radio transmitters. From an architectural perspective, metasurfaces can be coordinated with ISAC transmitters and receivers to jointly optimize beamforming, waveform design, and resource allocation for both functions.

In this context, the ISC group develops use cases, requirements, architectures, and enabling technologies for ISAC, targeting applications such as localization, environment monitoring, healthcare, transportation, and smart infrastructure [75]. ISC considers metasurfaces as a tightly integrated technology that enhances and extends the capabilities of existing communications infrastructure, rather than as a standalone sensing system.

Overall, the ISC approach is more macroscopic compared to ISG, focusing on higher-level but modular functions and single tasks that can be performed by a metasurface to the benefit of either a user or another network sub-system.

Finally, the **ETSI ISG NFV** focuses at an even higher level, and defines the architectural framework, interfaces, and management principles for virtualizing network functions on standardized cloud infrastructure. Network Function Virtualization NFV is an architecture concept in telecommunications and networking where network functions—that traditionally ran on

dedicated, proprietary hardware—are instead implemented as software running on standard (commodity) servers [76]. ETSI ISG NFV has investigated the case of managing RIS as an additional cloud computing resource.

In this aspect, metasurfaces are considered as a new type of NFV Infrastructure (NFVI) resource that extends the traditional compute–storage–network model toward programmable physical radio environments [76, ETSI GR NFV-EVE 023]. Specifically, ISG NFV treats metasurfaces as a physical network resource that can be onboarded, inventoried, and managed within the NFV framework, similarly to other infrastructure components, via the Physical Infrastructure Manager (PIM). Metasurfaces are seen as capable of enhancing coverage, signal quality, and network efficiency by actively controlling radio-wave propagation, effectively extending the radio access closer to end users. Two alternative integration models are defined. In the first model, metasurfaces are managed as infrastructure elements abstracted and exposed to the management system for orchestration and resource allocation. In the second model, metasurfaces are modeled as Physical Network Functions where a dedicated descriptor defines their connectivity and role. This body also highlights key management challenges, including the metasurface lifecycle management, monitoring (e.g., energy consumption), interaction with external controllers (often owned by third parties such as building owners), and defining clear demarcation points between the cloud management system and external network management systems.

VI. SIMULATING NETWORKED PWES: THE OMNET++ CASE

Simulators supporting metasurfaces at the physical layer have emerged, both commercial and open-source [77], [78]. Moreover, RIS-specific simulators have also appeared [79]. These tools operate on either ray-tracing or full-wave solver principles and provide signal quality indications, assuming that the metasurfaces in the system have been configured (i.e., after the optimization problem has been solved) and the user device parameters (such as directivity, power, sensitivity) have been set.

Conceptually, one could employ these tools within a heuristic optimization loop, executing simulations and improving upon the choice of EM Functions per tile. However this entails a computational burden that may not be generally sustainable, making these tools more fit for the final step of an evaluation, deducing more accurate results for an already optimized PWE configuration decision. (This also affects optimal metasurface deployment studies [63], which require an even larger simulation overhead).

It is for the same reason that these tools do not merge directly with network-layer concerns and simulations. However, network-layer simulators, such as NS, Omnet++ and OPNET are known to effectively cover wireless standards, employing more computationally scalable approaches, such link budget tools and statistical communication models [80]. Such approaches have already started to appear and gain momentum in the area of vehicular networks [46]. In the following, we

outline the process of incorporating metasurfaces into any discrete event simulator for networks, using Omnet++ as a driving example [81].

Prerequisites. The simulation design will rely on the PWE graph model. In this model, the EM Functions are well-defined, using the graph links as EM Function parameters as required. In general, a tile can treat any subset of its links as incoming wave directions, and any subset as departing wave directions. We define the following problems:

Problem 9. How does a graph-level EM Function translate to an actual EM performance? In other words, following the notation of Fig. 5, how does one obtain the efficiency degrees per departing wave direction?

Solution 10. Decompose each complex EM Function into simple ones, for which a codebook exists or that can be calculated in reasonable time. Each complex EM Function can be effectively decompose to multiple single steerings, if from one incoming link to one departing link. If a codebook exists for these single steerings, then the efficiency degrees for the complex function can be derived following the process described in the context of Fig. 4. Deriving the codebook for single steerings can be accomplished via existing standalone tools [82], [83].

Problem 11. What properties should a PWE graph have?

Solution 12. In general, several metasurfaces tiles are placed over walls and ceilings. These tiles are node graphs without connectivity. However, walls and ceilings composing a room comprise tile sets with extensive connectivity, as shown in Fig. 6. Further discussion on the topic can be found in Section VIII-A, while graph generation and visualization scripts can be found online [84].

Problem 13. How does a wave attenuate over a PWE graph?

Solution 14. Consider a path originating from a transmitter and ending at a receiver within a PWE graph, crossing N tiles and $N + 1$ links, effectively over N steering EM Functions. If the tiles can employ the collimation functionality (cf. Section III-A) in tandem with steering, then the received power will be (extending [46]):

$$P_r = \frac{P_t \epsilon_t \epsilon_r \prod_{n=1}^N \epsilon_n}{\prod_{n=1}^{N+1} \left(\frac{4\pi f}{c} \right)^2 \|l_n\|^{\alpha_n}} \cdot \prod_{n=1}^{N+1} L_n, \quad (10)$$

where P_t is the transmission power, ϵ_t and ϵ_r the antenna efficiency factors of the user devices along the directions of the first and the last link, ϵ_n is the EM Function efficiency at tile n , $\|l_n\|$ is the distance of the n^{th} link over the path, a_n is a factor expressing the path loss as affected by the efficiency of the collimation functionality and value of $\|l_n\|$, and L_n is any link loss stemming from partial LOS as stated in Remark 5 or 1 otherwise. (While a_n can be statistically derived by the physical-layer simulation tools, its value should be less than 2, which is the free space loss exponent. A rule of thumb would be to assume $a \approx 1$ near a tile and $a \approx 2$ in its far field).

When the tiles do not support collimation functionalities, then they essentially act as plain reflectors (albeit without mechanical movement). In this case, equation (10) is rewritten as [46]:

$$P_r = \frac{P_t \epsilon_t \epsilon_r \prod_{n=1}^N \epsilon_n}{\left(\frac{4\pi f}{c}\right)^2 \left(\sum_{i=1}^{N+1} \|l_n\|\right)^\alpha} \cdot \prod_{n=1}^{N+1} L_n, \quad (11)$$

where a is now uniform and takes a value of less than 2, as dictated by the type of the 3D setting [85].

Notably equations (10) and (11) can be combined accordingly when using mixed-technology metasurfaces within the same PWE.

Remark 15. Having a defined PWE graph and EM Functions (e.g., via the processes described in Section IV-C), as well as the user device parameters, one can traverse the PWE graph and derive the resulting approximate Power Delay Profile.

Omnet++ integration. As discussed in Section IV, the PDP is a set containing the power, latency, phase (and polarization) of each path reaching the receiver. It is noted that dedicated EM Functions can modify the phase and polarization of a wave, essentially attaining over the air path equalization and polarization matching, respectively. In any case, the PDP contains all the necessary information to derive the resulting bit error error rate and fading model, given a selected modulation scheme and a symbol duration and, hence, the attainable data transfer rate as well [86].

Therefore, PDP will act as the intermediate to interface the PWE world to the Omnet++ simulation engine.

Omnet++ comes tightly integrated with the INET/MANET framework, which contains an extensive set of protocols per OSI layer stack, including wireless propagation. The latter can be approached either:

- from the more abstract level of link budget and stochastic channel models (employing the classes `WirelessChannel`, `IRadio`, `RadioMedium`, `AnalogModel`, `Signal`, `PacketLevelRadio` vs. `AnalogRadio`, `PropagationLossModel`, `PathLoss`, `Fading`).
- from the more precise waveform-level of simulation, providing ways to simulate specific waveform encoding, decoding, modulation and distortion (employing classes such as `TransmissionBase`, `IRadioSignal` and `AnalogModelResult`).

Since we have motivated the need for computationally lighter simulations, the first approach is deemed as more fitting. In order to proceed with it an new type of channel needs to be expressed, which will capture the prerequisites listed above. This can be achieved by extending the `RadioMedium`, which will allow for:

- intercepting Omnet++ transmission events,
- transform the signal as dictated by the PWE graph, and finally
- deliver it to the receiver, creating a modified copies of the original `Transmission`/`Signal` object, in order to create the proper PDP.

Note that there are two approaches for modeling the PWE environment within Omnet++:

- 1) Keep only the user devices present within the INET network, while the actual tiles reside outside Omnet engine, providing a PDP that matches the EM Function choices upon callback.
- 2) Model both the users and the tiles within the INET network.

The first approach keeps most of the INET modeling approach intact and requires only the introduction of a rather minor class extension. Moreover, the existing tools for PWE graph generation, configuration and traversal can be exploiting directly via simple interfaces. Additionally, assuming that these Omnet-external tools can be called upon as services, a high degree of parallelism can be achieved, with Omnet++ calling upon multiple PWE graph configuration to evaluate in parallel, e.g., in terms of TCP-over-PWE performance.

The second approach calls for re-implementing existing tools within the Omnet++ codebase. It can offer a more mature approach in the long-term, as the ensuing modularity would allow for targeted code improvements and extensions, all exposed to the end user via the NED scripting language, which is employed by Omnet++ in order to create scenarios over an existing, compiled version of the INET/MANET framework.

An overview of the proposed implementation in UML format is given in Fig. 11. We consider the class `PWEModifierMedium` which extends `inet::physicallayer::RadioMedium`, intercepting the INET reception/delivery hooks. (E.g., `deliverPacketToChannel` / `deliverTransmissions` or `interceptTransmission` / `handleTransmission`).

Additionally, we introduce a custom singleton class called `PWEPolicy`, which is a data holder for the communication objectives per user in the system, as described in Section IV-A. When a user emits a signal, it is intercepted by the `PWEModifierMedium` and a lookup for corresponding objectives is made in the `PWEPolicy` instance. If no entry is found, the wireless propagation occurs with the PWE as-is (i.e., configures, partially configured or unconfigured, i.e., regular propagation).

If matching rules are found, then the simulation can either: greedily reconfigure the PWE via the external service, leaving the rest of the PWE configuration as-is, as a more lightweight simulation solution, or proceed to completely reconfigure the whole PWE for all users and user objectives. In any case, a PDP is produced which is passed to the Omnet++ engine and dictates the number and parameters of all copies of the original transmissions to be delivered to the Omnet++ receivers. All other OSI layers simulated by Omnet++ operate normally.

It is noted that, while many of the above specifics refer to Omnet++, the same logic—i.e., calling upon PWE graph processing utilities as external services—can be employed for other network simulators (e.g., NS or OPNET) by using a similar interception at the class representing the wireless propagation medium.

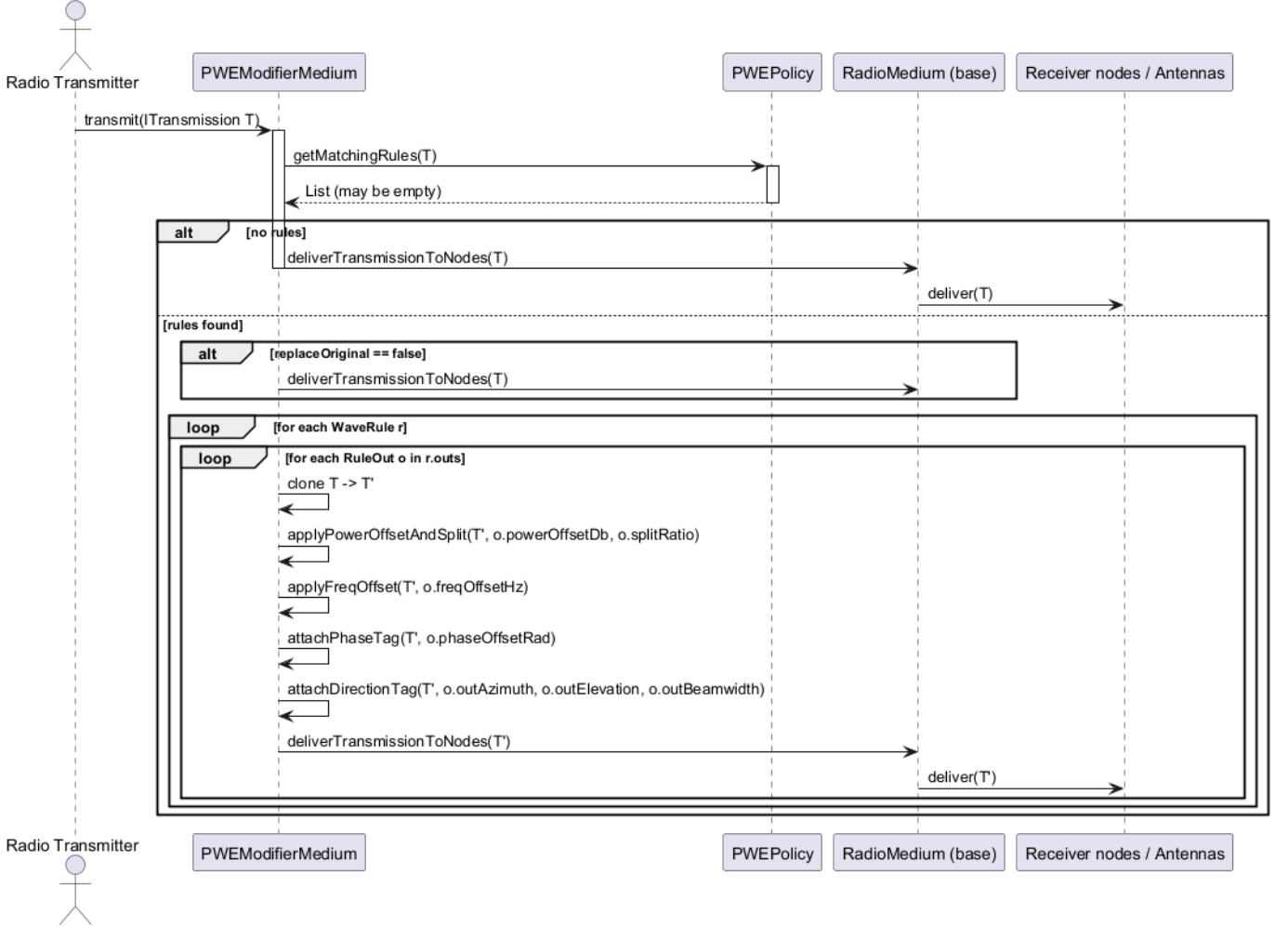


Figure 11: UML overview of the proposed PWE-Omnet++ integration.

VII. EVALUATION: A FACTORY APPLICATION EXAMPLE

One of the main use cases envisioned for PWEs are in the context of factory settings, exemplary shown in Fig. 12. These scenarios often have complicated wireless environments due to heavy production machinery or storage racks blocking signals. Instead of deploying multiple repeaters or access points, PWEs can be used to extend coverage to areas that would otherwise be out of the line of sight of the base station and, most importantly, mitigate propagation phenomena that could be detrimental to strict machinery requirements, such Computerized Numerical Control (CNC) equipment [87]. Such systems require communication time-sensitivity and near-zero error tolerance in their actuator-sensor control loops, especially when operating in orchestration with other equipment. Additionally, as the user devices in such environments often move on predetermined and scheduled paths, such as with robots taking items from one rack to another, it simplifies the measures required to control a PWE in real-time.

In a more concrete scenario, robots move on pre-scheduled routes to retrieve items from storage racks in a warehouse. They take these items and move them to an area where they will be packed for shipping. While the robots are moving,

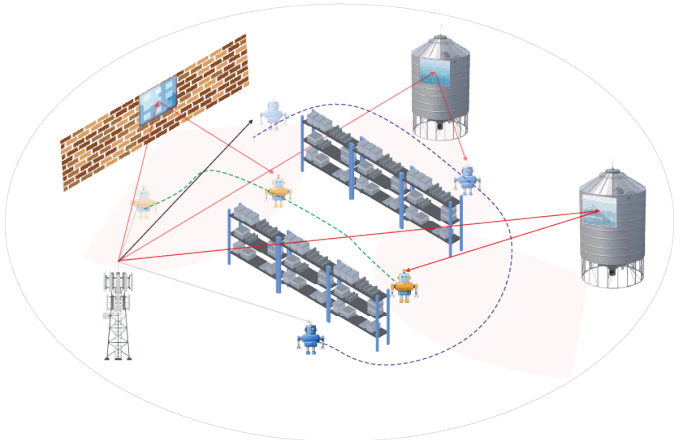


Figure 12: Conceptual application of a PWE in a factory setting.

they still need to stay connected to the network the entire time to transmit telemetry data as well as receive any possible updates to their routing etc. PWEs can be deployed to ensure that such constraints, and their networking requirements, are

Table IV: SIMULATION PARAMETERS

Ceiling Height	3 m
SDM Dimensions	1 × 1 m
SDM Design	[78]
Frequency	60 GHz
Tx Power	30 dBm
Tx/Rx Antenna types	Pyramidal horn, 80° beamwidth (pointing upwards)
Max ray bounces	50
Min considered ray power	-250 dBm

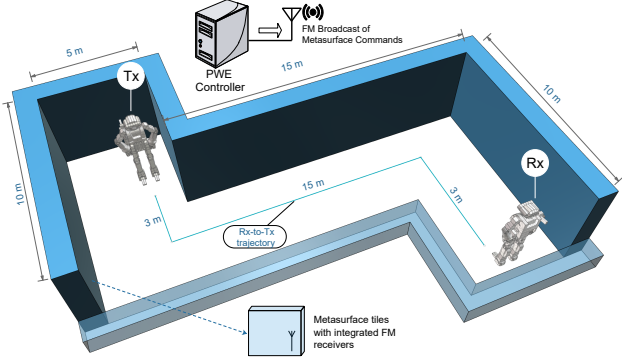


Figure 13: Overview of the employed simulation scenario.

met. Furthermore, as the robots are moving at high speeds, the metasurfaces can be used to reduce the Doppler effect that would otherwise occur, by ensuring that a wave meets the trajectory of a robot perpendicularly.

We proceed to study this setting in the following simulation, employing the path finding-driven heuristic outlined in Section IV-C1. Specifically, we employ the KPConfig heuristic and the associated simulation engine [8]. Physical-layer parameters are summarized in Table IV.

A. Simulation Scenario and Results

We proceed to examine the setup of Fig. 13, studying the segment of a symmetric Z-shaped corridor (dimensions are embedded in the Figure). All the walls and the ceiling are covered with metasurfaces specified in Table IV and scaled for operation in the employed mmWave frequency. Metasurfaces can be active and configured for an EM Function, in which case they operate per their physical design [78], or be deactivated and act as perfect reflectors.

A PWE server sends commands to the metasurface units using an FM broadcast channel supporting a data rate of 360 Kbps. (We note that this choice is made to accentuate the potential for cheap and massive control channel connectivity for metasurfaces in the context of this tutorial). Thus, each metasurface is equipped with a matching FM receiver. The PWE controller serializes and broadcasts the EM Function commands for each metasurface unit, each in the form of “preamble, metasurface id, EM Function id, Parameter 1, Parameter 2, ...” [20], thus creating a broadcast schedule. The schedule is concluded with a special message that notifies each metasurface to deploy its most recently read EM Function

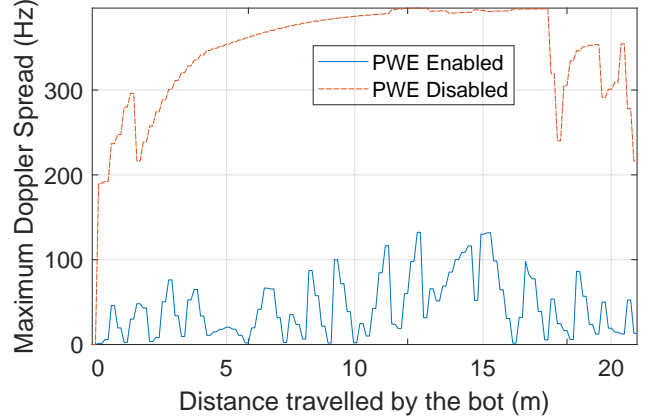


Figure 14: Maximum Doppler spread for the RX bot during its movement with PWE enabled/disabled.

from the FM stream. The total size of the schedule is considered to be 360 Kb, accounting for up to 1000 metasurfaces and 360 bits per single metasurface command. Notice that each metasurface is considered to self-host the information required to map the broadcast EM Function identifier and the associated parameters to the corresponding embedded circuit element states.

Two robots communicate at the mmWave range, while the Rx moves along a well-defined trajectory with a steady speed of 1 m/s. The PWE is tasked with mitigating the Doppler spread, while also maximizing the received power at the Rx. The exact nature of the robot communication in terms of application scenario goes beyond the scope of this tutorial and is left undefined. Notably, the Rx robot trajectory is highly predictable. Once the robot announces its movement characteristics (trajectory, speed) and initiation to the PWE controller, and considering its initial park position to be known as well, the PWE controller can infer its position at any given time moment required. Thus, the broadcast schedule contains commands that will be matching the bot’s position at the moment when the deploy signal is emitted. Finally, both bots have their antennas pointing upwards, in order to: i) ensure that there is contact with metasurface units, and ii) there is no strong LOS component, which would be unmanageable by the PWE.

We proceed to examine the attained maximum Doppler spread in Fig. 14.

With the PWE disabled, the spread is nearly constantly at 400 Hz. This is especially notable in the 5 m → 10 m traveled distance, where the bot enters and exists the corridor respectively, and the RF waves reach its trajectory head on.

Notably, with the PWE enabled, the spread values remain below 120 Hz throughout the bot’s movement, and on average at 70 Hz. A spiking behavior is noted, with jumps from ≈ 0 Hz to 120 Hz. These repeat approximately every 1 m, and essentially follow the “freshness” of the deployed EM Functions, which are refreshed every 1 sec, considering the 360 Kb schedule size, the 360 Kbps FM broadcast rate and the 1 m/s bot speed. Additional parameters affecting the overall form of the plot are the efficiency degree of the

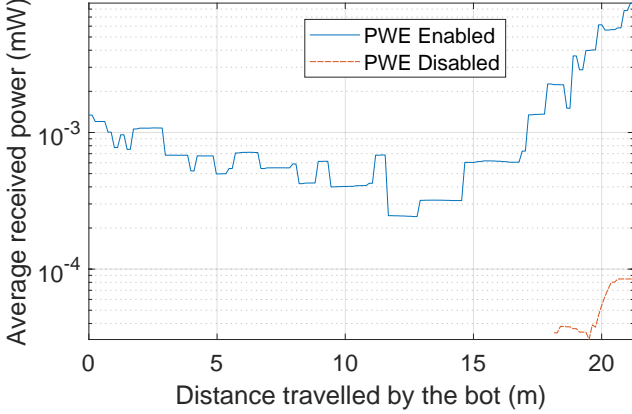


Figure 15: Average received power for the RX bot during its movement with PWE enabled/disabled.

PWE optimization process, which can also be subject to the geometry of the space and the placement of the tiles.

Figure 15 shows the received power across the bot’s trajectory, with the PWE enabled and disabled. In the latter case, the Rx bot does not receive notable power during its movement, apart from the last part of its trajectory, when the distance to the Tx has become minimal. This is aligned with the challenging nature of the mmWave communications.

When the PWE becomes enabled, the Rx bot receives power throughout its movement. Notably, the received power drops up to a point near the middle of corridor, and then increases once more, due to the Tx-Rx distance reduction. This behavior at the middle of the movement is due to the fact that less metasurface units are in close proximity to the Rx bot at this point. As such, the EM waves cannot be as effectively handled as, e.g., at the initial bot position, where it is effectively surrounded by metasurface units.

This exemplary scenario aimed at demonstrating the network/PWE interplay and the effect on the communication quality, while also studying traits that can only be offered by metasurface-driven setups, i.e., Doppler spread mitigation and coverage extension in the mmWave. Notably, real-world industrial setups may be able to offer lower-latency control than the simple FM broadcast approach employed here, at a perhaps increased overall cost. However, apart from the aforementioned interplay study, it is noted that PWEs should be easily deployable and extensible at scale, favoring their adoption and deployment in existing spaces.

VIII. DISCUSSION AND NETWORK RESEARCH DIRECTIONS

We proceed to outline research challenges from the aspects of graph analysis, networking, integration and machine learning.

A. Graph theoretic challenges

As discussed in Section IV-A, the optimal configuration of a PWE necessitates the graph exploration and exploitation of

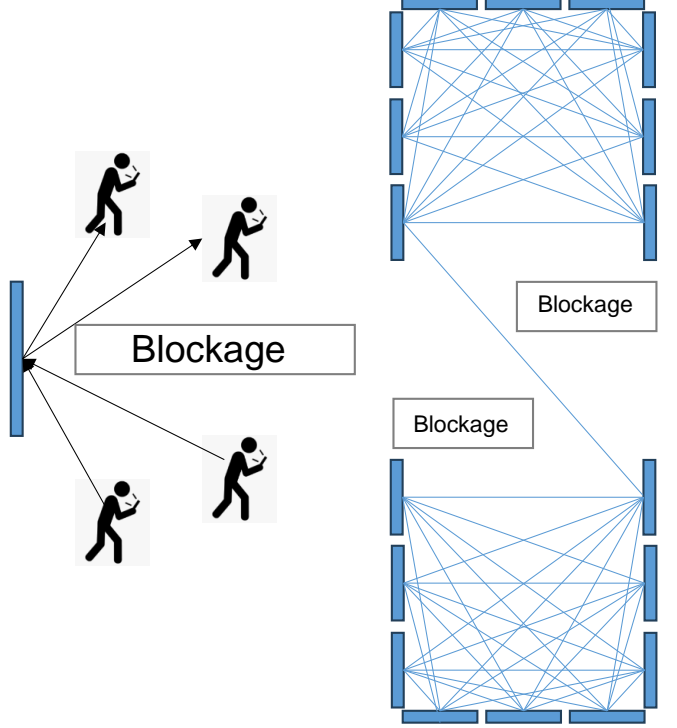


Figure 16: Visualization of the properties of symmetry (left), clique and min-cut (right) of the PWE graph.

its properties. In this context we outline two major research challenges as follows.

Exploitation of key-graph properties. As shown in Fig. 16, there exist some graph properties that call for exploitation and facilitate the PWE configuration. In particular:

- The symmetry property, i.e., the existence of nodes that act as natural or metasurface “mirrors”, i.e., without or with the use of an EM Function, respectively, for a set of neighboring nodes. Such nodes allow for the deployment of a single EM Function that perfectly serves many connectivity paths, without suffering from any loss in efficiency that would stem from merging multiple steering EM Functions. Such tiles can be required to act as waypoints, maximizing the number of free tiles within the PWE after a full configuration.
- The existence of cliques (either in the strict or in the approximate sense) in a PWE graph is expected to be a frequently recurring property. As tiles are placed on walls and ceilings in rectangular rooms, each tile can be deemed connectable to all other tiles, apart from the co-planar ones. Thus, any tile can act as a room/clique “representative” in an initial routing phase, and then favoring the stochastic path exploration by delegating connectivity to any other tile around it.
- The existence of min-cuts is also a useful property, as they define PWE graph links (and tiles at their endpoints) that provide critical connectivity to different parts of the graph. As such, they should undergo significant EM Function optimization, and checks for symmetry properties, in order to serve as many disparate user

objectives as possible, with minimal efficiency loss due to EM Function merging.

Beyond these indicative properties, a thorough examination of additional ones and their relation to the PWE configuration is considered a major open challenge.

Graph path finding for PWE graphs. Computer networking, along with multitude other disciplines, has made extended use of path finding algorithms. Tools such as A*, Dijkstra's algorithms and K-Paths are being proven immensely useful in routing and traffic engineering. However, these tools and many other covering cases of dynamic graphs, have one common property: the graph nodes are re-entrant in the sense that any path finding process that finds itself at a node will see the same link outgoing links and weights.

The PWE graph is peculiar in the sense that this property no longer holds. For instance, consider a node configured for steering from one adjacent link to another. If the path exploration process enters the same node from an unintentional arrival link, it may find a completely different outgoing weight (due to lower efficiency towards unintended EM Function inputs) and even complete lack of subsequent connectivity. As such, the existing path finding tools acquire an indicative value in terms of their outputs. In other words, a multitude of paths are first found and then evaluated in terms of service to the PWE configuration.

In this aspect, a challenge is to revisit these classic aforementioned tools and imbue them with compatibility for non re-entrant graphs. Alternatively, new link weight definitions can be engineered in order to increase the usefulness of the outputs of classic path finding tools.

B. Networked PWE Challenges

As demonstrated in Section VII, the interplay between the network control and the PWE is decisive to the performance levels that the users receive. As such, we define the following challenges related to proactive traffic engineering, low-latency control and network architecture.

Traffic engineering and PWEs. Traffic engineering is the process of distributing the traffic over a network in a manner that fulfills performance criteria and makes the network more robust to strain, such as denial of service attacks and outages due to hardware impairments. In the context of PWEs, similar techniques must be enforced to strengthen the isolation of user groups and ensure a high-level of performance under user mobility.

Two exemplary challenges are visualized in Fig. 17:

The top part illustrates a user receiving strong signal from a tile, while an eavesdropper has aligned himself to the user's direction of service. A sudden displacement of the user, coupled with low network reaction times, can expose his signal to the eavesdropper, while also sharply reducing the user's wireless reception strength. This can be considered a case that calls for proactive mitigation at the last-hops of the air paths assigned to the user. First, signals must be routed to the immediate vicinity of the user, to ensure connectivity. Second, the paths must either follow improbable directions of arrival (e.g., from the ceiling), or take into account the relative position of other users in the general vicinity.

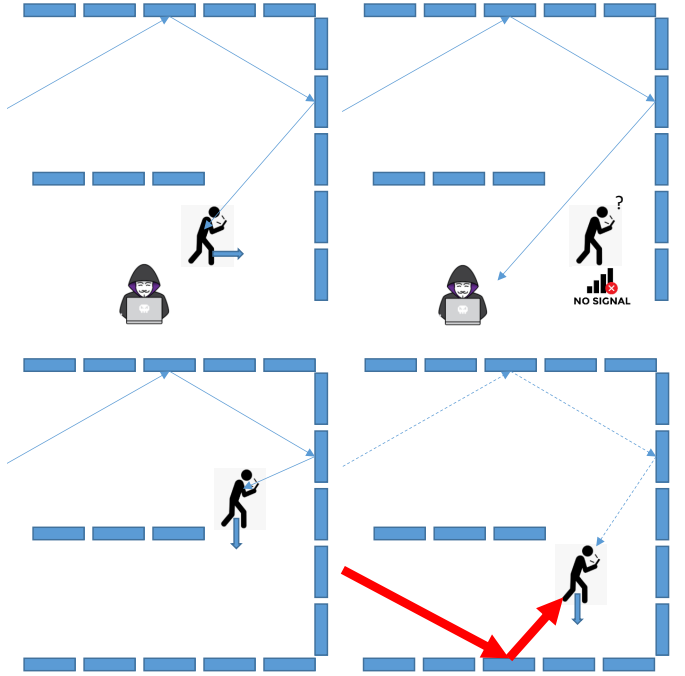


Figure 17: Visualization of PWE configuration challenges to be mitigated by proactive traffic engineering. Top: passive eavesdropping by aligning to the user's direction of service. Bottom: massive PWE reconfiguration owed to user displacement.

The bottom part illustrates a case that calls for strategic, full-path engineering. A user that is being serviced by a major PWE path suddenly moves to another room, where the same path attenuates beyond use. Should the PWE routing tree adapt reactively, a considerable amount of time may elapse before the connectivity is restored. A proactive policy could, e.g., have already deployed secondary paths that offer a smooth handover.

Interfacing with existing low-latency networking efforts. Managing the control and orchestration of metasurfaces within heterogeneous network environments poses interesting technical and theoretical challenges (HetNet [88]). The seamless integration of metasurfaces requires advanced control-plane algorithms that can efficiently coordinate between metasurface elements and existing base stations while ensuring optimal performance within a time-sensitive networking (TSN) framework [89]. This also necessitates the development of sophisticated management protocols that can operate in real-time.

Another framework of interest is the Age of Information (AoI) which promotes the concept of information freshness [90]. According to it, the reading from a sensor loses its significance following a utility function defined over the time elapsed since the last measurement. Returning to the evaluation example of Fig. 14, it is evident that information freshness plays a significant role to the PWE performance, hinting prospects for an analysis that quantifies it and an ensuing optimization.

PWE control architecture. In the evaluation scenario, we employed a cost-effective broadcast push type of PWE control

employing FM radio. Within this context, we employed a flat broadcast schedule (also known as round-robin) to post directives to each tile. Notable, there exist techniques for performing push schedule optimization by increasing the number of commands for specific tiles within a single schedule, in order to adapt to, e.g., a rapidly changing RF environment within a specific room [91]. This can decrease the control latency of push-based solutions while retaining their cost-effectiveness. Apart from push-based control, on-demand non-periodic broadcast scheduling techniques can be employed as well, with the trade-off of requiring a two-way lightweight communication with the tiles [92]. Additionally, the broadcast nature of control can also be attained over wired bus architectures.

Finally, apart from a centralized control solution, there exist emerging metasurface technologies that also enable them to act autonomically and based on local input [93], thus allowing for a distributed (i.e., server-less) PWE control architecture. Such metasurfaces employ autonomous impinging wave sensing, while their overall orchestration can be seen as a distributed control challenge based, e.g., on consensus schemes for deducing the optimal PWE-wide RF behavior [94].

C. Standardization and Integration Challenges

The integration of metasurfaces into existing networks presents many open challenges, as is evident by the state of the standards, summarized in Table V. Notice that the standardization and regulatory framework surrounding metasurfaces is in the state of preparing the necessary foundations (ETSI), or plainly informative (3GPP). Since the technology is still emerging, there is significant innovation potential towards their deployment and interoperability with existing network infrastructures. Establishing efficient solutions and frameworks per aspect (cf. Table V) is essential for facilitating a smooth integration process. A unified treatment from the standardization bodies is also in need as, for instance, ETSI views metasurfaces as a network resource, while 3GPP as a part of the RF environment only, as shown in Table V.

Nonetheless, the deployment focus on 5G-Advanced and beyond-6G networks introduces challenges in terms of resource management and optimization strategies. How to effectively incorporate metasurfaces into evolving network architectures while maintaining compatibility with past and future technologies is a critical challenge that researchers and stakeholders must jointly address. In this aspect, it would be beneficial to align PWEs with existing resource allocation approaches, providing extensions of related frameworks, rather than requiring completely novel solutions.

In this aspect we highlight the close relation between the PWE optimization and the concept of Virtual Network Embedding (VNE) [95], which also relates to the NFV standardization actions covered in Section V-B, as well as the concept of microservices [96]. In general, VNE is a process within network virtualization that allows multiple isolated virtual networks to be deployed on a single physical infrastructure, enhancing resource efficiency. This method involves mapping virtual components, such as virtual machines or containers, onto physical network elements like servers and switches.

The VNE process typically begins with designing the virtual network topology based on specific requirements. For instance, a company deploying a cloud-based application might create a virtual network topology consisting of three VMs connected by a virtual switch. These VMs are then assigned to different physical servers using a virtual switch implemented on the physical switches. The algorithms that perform this assignment first decide whether an embedding request is admissible to the physical infrastructure, i.e., whether there exist resources to serve it. A greedy, coarse mapping phase is initiated, where the most demanding virtual resources are mapped to the most under-utilized but collocated physical resources. Stochastic search is performed to deduce the final mapping that fulfills any performance conditions.

As noted in Sections IV-A and IV-C, the PWE optimization bears strong similarity to this workflow. The user connectivity requirements (e.g., connect to a set of users and an access point) can be viewed as an embedding request for a corresponding virtual network, with the notable difference that the user locations are known, acting as anchors to the VNE mapping phase. An open challenge is to provide concrete VNE algorithmic extensions that bridge the two concepts completely. In this aspect, separate directions can focus on: resource optimization, which is a key benefit of VNE, as it enables efficient use of physical infrastructure resources; scalability, allowing new services or applications to be added without investing in additional hardware; flexibility permitting diverse network designs on the same infrastructure; isolation, which is crucial for security, ensuring that a compromise in one virtual network does not affect others; simplified network manageability by providing a logical view of the network separate from the physical infrastructure, making it easier to monitor and manage.

Moreover, a related concept is that of dependent microservices. This follows the VNE rationale, yet it considers not VMs but interdependent services that need to be: i) mapped to a physical infrastructure, and ii) form a workflow over a data stream that traverses them. For instance, one microservice can act as firewall, passing on the stream to a web server. In this aspect, let EM Functions be "microservices". The alignment concept can be to: i) offer what the user needs (e.g., alter the phase, correct the polarization, etc., each can be a single "microservice" that can run anywhere over a path), and ii) keep the overall number of microservices--e.g., steerings--over each path minimal. Additionally, the EM microservices can affect each other unintentionally (a wave "leaking" can cause unintended effects), so the chosen tiles to host these "microservices" (per user pair) should also have a degree of distance from microservices that will be used for other user pairs.

Additionally, there are several challenges that need to be faced when trying to integrate PWEs into existing radio access network (RAN) architectures [97]. These challenges largely dictate which integration scenario for PWEs is feasible. These range from transparent, i.e. no other network component is aware of the existence of the PWE, to full coordination where the PWE is fully integrated. Depending on the level of coordination different scenarios can be supported. The main

Aspect	ETSI ISG RIS	3GPP (up to release 19)
Standardization status	Dedicated ISG fully focused on RIS	No dedicated Work Item
Metasurface definition	Explicitly defined entity	Not formally defined
Architectural role	Metasurfaces as network resource	Metasurfaces as part of the RF environment
Control & management	Control, orchestration, and lifecycle studied	No control-plane specification
Channel models	RIS-specific near-far-field models	Generic channel models
Use cases	Communications, sensing, localization, ISAC	Discussed only at vision/study level
Deployment focus	5G-Advanced and 6G	Mainly beyond-5G / 6G vision
Normative intent	Preparing foundation for future specs	Informative references only

Table V: Comparison of ETSI ISG RIS and 3GPP Standards

challenges involve user device tracking, switching between a PWE and a direct connection, multiplexing multiple user devices that are connected to the same PWE, as well as beam leaps, where a device moves out of the LOS of the base station and connects to PWE, leading to a sudden "jump" in its location from the perspective of the base station. While static single device use-cases face none of these challenges, scenarios in which multiple mobile devices with intermittent LOS exist would face all of them.

Accordingly, the more complex the scenario, the more tightly integrated the PWE has to be. The main trade-off here comes in the form of protocol extensions: While a transparent PWE can just be deployed without the need to change the architecture at all, a fully integrated one would require a thorough rework of the existing standards. For example, an extension to the Open RAN alliance (ORAN) architecture would involve the addition of at least one new interface and changes to several of the controllers. While this is not entirely unfeasible, it is a significant hurdle to large scale PWE deployments. As such, in any upcoming standardization attempts, a balance needs to be struck between which use cases to support and how many changes and extensions to make to the specifications.

D. AI-driven Applications and Challenges

While AI can act as a facilitator for the aforementioned challenges, it can also act as an enabler for further applications on its own. While potential metasurface applications such as communications, localization, and sensing are recognized, further research is needed to explore their practical implications and to define clear use cases that justify the investment in the metasurface technology. Thus, novel applications merge AI and PWEs to create systems that perform 3D monitoring of objects—a type of RF tomography—including their material composition in real-time [98].

The operating principle is shown in Fig. 18: i) Programmable metasurfaces are employed to create an optimal radio-frequency interaction between electromagnetic waves and an arbitrary object. ii) Radiofrequency imaging theory principles are employed to deduce the contribution of the wireless wavefront features (received by an array of antennas) to the 3D visualization of an object. iii) Following a training-validation phase, an AI system directly translates the received wavefront to 3D graphics.

The offered advantages of this approach are that: i) Real object rotations can be automatically transformed to rotations of its 3D representation in real-time, without the need for

computer computations, motion sensors and lidars, and ii) The internal structure of the object is also revealed, allowing for a type of RF tomography that is privacy preserving, has real-time operation prospects, and does not employ ionizing radiation. Notice that the use of AI as the RF-to-graphics converter is classified as a non-linear process, whose fidelity bounds are not explored, contrary to linear processes and their well-known limitations [99].

IX. CONCLUSION

This tutorial explored the concept of controlling metasurfaces from a network-centric perspective. By treating metasurfaces as specialized network components, it was shown how network theory can provide new insights into their design, optimization, and integration with existing infrastructure.

The paper reviewed the physical principles of metasurfaces and their various applications, followed by an exploration of manufacturing approaches. Subsequently, it was shown that modeling metasurfaces as wave routers allows for describing systems of metasurfaces using graph theory. This approach enabled the development of a performance objective framework for optimizing these systems, with simplifications leveraging heuristic and path-finding algorithms.

The paper also examined the integration of metasurfaces into communication systems, discussing their overall workflow and examining their interface with existing wireless systems from the standardization point of view, as well as by discussing simulation prospects via existing network discrete event simulators. An evaluation example showcasing the mitigation of the Doppler spread in a mmWave setting provided a demonstration of the PWE potential as well as a basic simulation setting for further experimentation.

Finally, the paper explored future directions for research in this field, identifying graph-theoretic challenges, networked PWE challenges, and standardization and integration challenges. We also considered the potential of AI-driven applications, towards application beyond the strict context of data exchange.

REFERENCES

- [1] C. Liaskos, A. Tsoliaridou, A. Pitsillides, S. Ioannidis, and I. Akyildiz, "Using any surface to realize a new paradigm for wireless communications," *Communications of the ACM*, vol. 61, no. 11, pp. 30–33, 2018.
- [2] O. A. Abdelraouf, Z. Wang, H. Liu, Z. Dong, Q. Wang, M. Ye, X. R. Wang, Q. J. Wang, and H. Liu, "Recent advances in tunable metasurfaces: materials, design, and applications," *ACS nano*, vol. 16, no. 9, pp. 13 339–13 369, 2022.
- [3] C. Liaskos *et al.*, "A New Wireless Communication Paradigm through Software-controlled Metasurfaces," *IEEE Communications Magazine*, vol. 9, pp. 162–169, 2018.

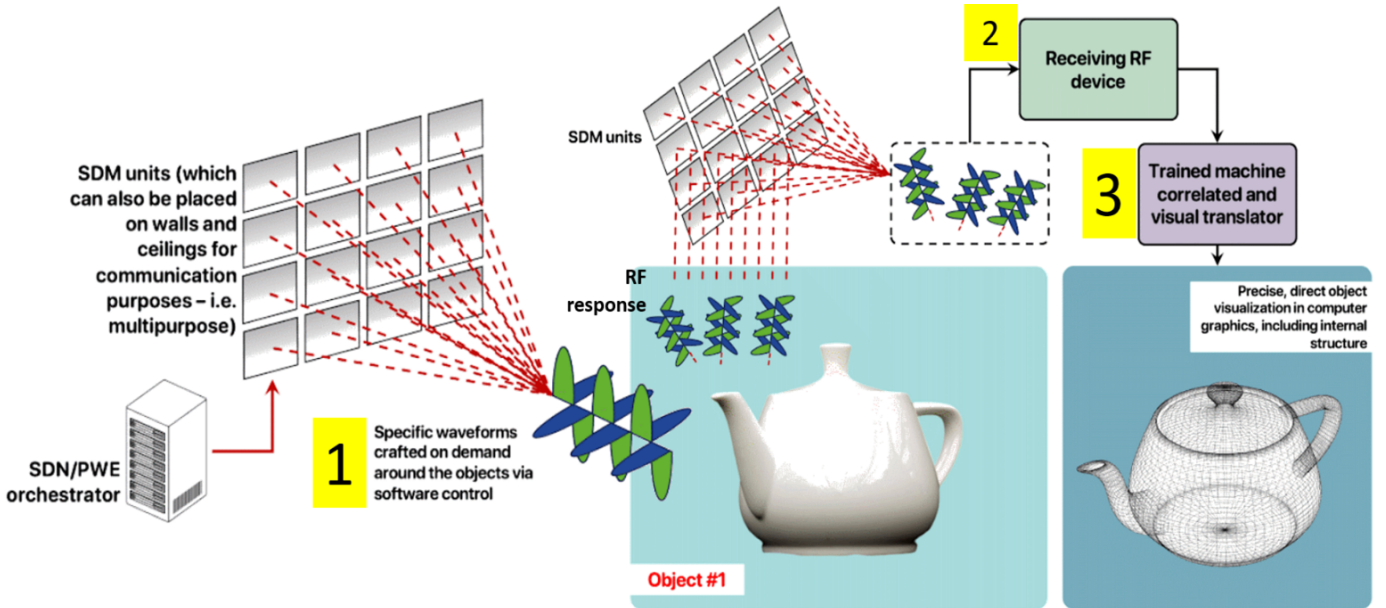


Figure 18: Principles of the envisioned AI-PWE driven RF tomography.

- [4] A. Welkie *et al.*, “Programmable radio environments for smart spaces,” in *ACM HOTNETS’17*, pp. 36–42.
- [5] S. Han and K. G. Shin, “Enhancing wireless performance using reflectors,” in *IEEE INFOCOM 2017-IEEE Conference on Computer Communications*. IEEE, 2017, pp. 1–9.
- [6] X. Tan, Z. Sun, J. M. Jornet, and D. Pados, “Increasing indoor spectrum sharing capacity using smart reflect-array,” in *2016 IEEE International Conference on Communications (ICC)*. IEEE, 2016, pp. 1–6.
- [7] N. Kaina, M. Dupré, G. Lerosey, and M. Fink, “Shaping complex microwave fields in reverberating media with binary tunable metasurfaces,” *Scientific reports*, vol. 4, no. 1, p. 6693, 2014.
- [8] C. Liaskos, A. Tsoliariadou, S. Nie, A. Pitsillides, S. Ioannidis, and I. Akyildiz, “On the network-layer modeling and configuration of programmable wireless environments,” *IEEE/ACM Trans. Netw.*, vol. 27, no. 4, pp. 1696–1713, 2019.
- [9] K. Soukoulis and S. H. Fan, “Metalens: a new paradigm for optical imaging, communication, sensing and imaging,” *IEEE Transactions on Antennas and Propagation*, vol. 58(2), no. 2, pp. 357–365, 2010.
- [10] N. A. Engheta and P. Lande, “Effective negative refractive index,” *Physical Review Letters*, vol. 95(10), no. 10, p. 107401, 2005.
- [11] F. Zhang and S. H. Fan, “Experimental verification of the negative refractive index using metamaterials,” *Nature Materials*, vol. 7(1), no. 1, pp. 23–28, 2008.
- [12] L. Solymar and E. Shamonina, *Waves in metamaterials*. Oxford University Press, 2009.
- [13] T. Bao, H. Wang, H.-C. Yang, W.-J. Wang, and M. O. Hasna, “Performance analysis of ris-aided communication systems over the sum of cascaded rician fading with imperfect csi,” in *2022 IEEE Wireless Communications and Networking Conference (WCNC)*. IEEE, 2022, pp. 399–404.
- [14] R. Deng, B. Di, H. Zhang, Y. Tan, and L. Song, “Reconfigurable holographic surface: Holographic beamforming for metasurface-aided wireless communications,” *IEEE Transactions on Vehicular Technology*, vol. 70, no. 6, pp. 6255–6259, 2021.
- [15] X. Wang, F. Zhang, and S. H. Fan, “High-efficiency visible light source with a micro-lens metastructure,” *Optics Express*, vol. 20(12), no. A1208–A1216, 2012.
- [16] M. Xu, F. Zhang, and S. H. Fan, “Optical resonance of a metasurface at the nanoscale: A new paradigm for optical materials,” *Journal of Optics*, vol. 11(10), no. R57-R66, 2009.
- [17] F. Zhang and S. H. Fan, “Ultra-high numerical aperture in an optical system with a meta-material-based super-resolution lens,” *Optics Express*, vol. 20(12), no. A1217–A1224, 2012.
- [18] J. Lee, H. C. Kwon, S. K. Kim, Y. C. Lee, W. I. Park, T. M. Kim, Y. H. Yang, and B. G. Lee, “Metamaterial-based electromagnetic absorbers for radiation cooling applications,” *IEEE Transactions on Antennas and Propagation*, vol. 57(11), no. 11, pp. 3418–3425, 2009.
- [19] A. Liu, Z. Huang, M. Li, Y. Wan, W. Li, T. X. Han, C. Liu, R. Du, D. K. P. Tan, J. Lu *et al.*, “A survey on fundamental limits of integrated sensing and communication,” *IEEE Communications Surveys & Tutorials*, vol. 24, no. 2, pp. 994–1034, 2022.
- [20] C. Liaskos, *The Internet of Materials*. CRC Press, ISBN 978-0-367-45738-9, 2020.
- [21] F. Zhang *et al.*, “Lithography and etching for metamaterials,” *Journal of Photonic Nanoengineering*, vol. 8(2), no. S20-S34, 2015.
- [22] M. Li *et al.*, “Nanoimprint lithography for metamaterials,” *IEEE Transactions on Nanotechnology*, vol. 18(1), no. 1, pp. 53–62, 2019.
- [23] Y. Wang *et al.*, “Three-dimensional printing of electromagnetic metasurfaces,” *Optics Express*, vol. 25(15), no. A1241–A1252, 2017.
- [24] J. S. Huang *et al.*, “Varactor-based phase modulator using a graphene-based structure,” *Optics Express*, vol. 22(19), no. A1266–A1273, pp. A1266–A1273, 2014.
- [25] S. Atabak *et al.*, “Microelectromechanical systems for metamaterials,” *IEEE transactions on microwave theory and techniques*, vol. 63(10), no. 10, pp. 3228–3236, 2015.
- [26] W. Chen *et al.*, “Liquid crystal-based phase modulator for tunability across a wide frequency range,” *Optics Express*, vol. 27(11), no. A1041–A1052, pp. A1041–A1052, 2019.
- [27] Y. Wang *et al.*, “Graphene-based phase shifter using electrical tuning,” *IEEE Transactions on Electron Devices*, vol. 64(10), no. 10, pp. 2553–2562, 2017.
- [28] F. Zhang *et al.*, “Ferroelectric phase modulator for high-speed switching applications,” *Journal of Photonics and Nanoengineering*, vol. 8(2), no. 2, pp. S20–S34, 2015.
- [29] M. Li *et al.*, “Mechanically reconfigurable phase shifter using a micro-machined structure,” *IEEE Transactions on Nanotechnology*, vol. 18(1), no. 1, pp. 53–62, 2019.
- [30] D. Manessis, M. Seckel, L. Fu, O. Tsilipakos, A. Pitilakis, A. Tasolamprou, K. Kossifos, G. Varnava, C. Liaskos, M. Kafesaki *et al.*, “Manufacturing of high frequency substrates as software programmable metasurfaces on pcbs with integrated controller nodes,” in *2020 IEEE 8th Electronics System-Integration Technology Conference (ESTC)*. IEEE, 2020, pp. 1–7.
- [31] J. Sanz-Robinson, T. Moy, L. Huang, W. Rieutort-Louis, Y. Hu, S. Wagner, J. C. Sturm, and N. Verma, “Large-area electronics: A platform for next-generation human-computer interfaces,” *IEEE Journal on Emerging and Selected Topics in Circuits and Systems*, vol. 7, no. 1, pp. 38–49, 2016.
- [32] S. Yuvaraja, M. I. Nugraha, Q. He, L. R. Solay, P. A. Miranda Cortez, N. Xiao, M. Heaney, T. D. Anthopoulos, and X. Li, “Three-dimensional integrated hybrid complementary circuits for large-area electronics,” *Nature Electronics*, vol. 8, no. 10, p. 969–980, Oct. 2025. [Online]. Available: <http://dx.doi.org/10.1038/s41928-025-01469-0>

[33] K. Roy *et al.*, "Field-programmable gate arrays (fpgas): A survey," *IEEE Transactions on Very Large Scale Integration (VLSI)*, vol. 22, no. 2, pp. 141–155, 2014.

[34] H. Ishihara *et al.*, "Reconfigurable hardware for wireless networks: A survey," *ACM Computing Surveys (CSUR)*, vol. 45, no. 3, pp. 1–33, 2012.

[35] M. P. Cusack *et al.*, "Microcontrollers for the internet of things," *IEEE Transactions on Industrial Electronics*, vol. 64, no. 5, pp. 3429–3438, 2017.

[36] J. L. Bixby *et al.*, "Asic design and development: A survey," *Journal of VLSI Signal Processing: Systems for Signal Processing*, vol. 78, pp. 1–17, 2016.

[37] P. R. Martin *et al.*, "Digital signal processors for wireless communications," *IEEE Transactions on Wireless Communications*, vol. 14, no. 12, pp. 6404–6413, 2015.

[38] S. J. Kim *et al.*, "Mixed-signal design of high-speed data converters," *IEEE Journal of Solid-State Circuits*, vol. 48, no. 10, pp. 2301–2311, 2013.

[39] R. V. Joshi *et al.*, "System-on-chip (soc) design: A survey," *ACM Computing Surveys (CSUR)*, vol. 47, no. 4, pp. 1–31, 2015.

[40] D. Tyrovolas, S. A. Tegos, V. K. Papanikolaou, Y. Xiao, P.-V. Mekikis, P. D. Diamantoulakis, S. Ioannidis, C. K. Liaskos, and G. K. Karagiannidis, "Zero-energy reconfigurable intelligent surfaces (zeris)," *IEEE Transactions on Wireless Communications*, vol. 23, no. 7, pp. 7013–7026, 2023.

[41] N. M. K. Chowdhury, M. R. Rahman, and R. Boutaba, "Virtual network embedding with coordinated node and link mapping," in *IEEE INFOCOM 2009*. IEEE, 2009, pp. 783–791.

[42] H. Cao, S. Wu, Y. Hu, Y. Liu, and L. Yang, "A survey of embedding algorithm for virtual network embedding," *China Communications*, vol. 16, no. 12, pp. 1–33, 2019.

[43] A. Fischer, J. F. Botero, M. T. Beck, H. De Meer, and X. Hesselbach, "Virtual network embedding: A survey," *IEEE Communications Surveys & Tutorials*, vol. 15, no. 4, pp. 1888–1906, 2013.

[44] V. Sasikala and K. Chitra, "All optical switching and associated technologies: a review," *Journal of Optics*, vol. 47, no. 3, pp. 307–317, 2018.

[45] M. Pishvar and R. L. Harne, "Foundations for soft, smart matter by active mechanical metamaterials," *Advanced Science*, p. 2001384, 2020.

[46] M. Segata, P. Casari, M. Lestas, A. Papadopoulos, D. Tyrovolas, T. Saeed, G. Karagiannidis, and C. Liaskos, "Cooperis: A framework for the simulation of reconfigurable intelligent surfaces in cooperative driving environments," *Computer Networks*, vol. 248, p. 110443, 2024.

[47] A. Papadopoulos, D. Tyrovolas, A. Lalas, K. Votis, S. Schmid, S. Ioannidis, G. K. Karagiannidis, and C. K. Liaskos, "On modeling the ris as a resource: Multi-user allocation and efficiency-proportional pricing," *IEEE Transactions on Network and Service Management*, 2025.

[48] J. Lindsey, "The fresnel zone and its interpretive significance," *The Leading Edge*, vol. 8, no. 10, pp. 33–39, 1989.

[49] A. F. Molisch, *Wireless communications*. John Wiley & Sons, 2012, vol. 34.

[50] W. Kellerer, P. Kalmbach, A. Blenk, A. Basta, M. Reisslein, and S. Schmid, "Adaptable and data-driven softwarized networks: Review, opportunities, and challenges," *Proc. IEEE*, vol. 107, no. 4, pp. 711–731, 2019.

[51] K. He, J. Khalid, A. Gember-Jacobson, S. Das, C. Prakash, A. Akella, L. E. Li, and M. Thottan, "Measuring control plane latency in sdn-enabled switches," in *SOSR*. ACM, 2015, pp. 25:1–25:6.

[52] K. Foerster, S. Schmid, and S. Vissicchio, "Survey of consistent software-defined network updates," *IEEE Commun. Surv. Tutorials*, vol. 21, no. 2, pp. 1435–1461, 2019.

[53] M. Henzinger, A. Paz, A. Pourdamghani, and S. Schmid, "The augmentation-speed tradeoff for consistent network updates," in *SOSR*. ACM, 2022, pp. 67–80.

[54] S. Dudycz, A. Ludwig, and S. Schmid, "Can't touch this: Consistent network updates for multiple policies," in *DSN*. IEEE Computer Society, 2016, pp. 133–143.

[55] C. E. Miller, A. W. Tucker, and R. A. Zemlin, "Integer programming formulation of traveling salesman problems," *J. ACM*, vol. 7, no. 4, pp. 326–329, 1960.

[56] S. De Sirisuriya, T. Fernando, and M. Ariyaratne, "Algorithms for path optimizations: a short survey," *Computing*, vol. 105, no. 2, pp. 293–319, 2023.

[57] E. Q. V. Martins, "On a multicriteria shortest path problem," *European Journal of Operational Research*, 1984.

[58] R. E. Korf, "Artificial intelligence search algorithms," in *Algorithms and Theory of Computation Handbook*, ser. Chapman & Hall/CRC Applied Algorithms and Data Structures series. CRC Press, 1999.

[59] S. Luke, *Essentials of Metaheuristics*, 2nd ed. Lulu, 2013.

[60] C. Liaskos, S. Nie, A. Tsoliariadou, A. Pitsillides, S. Ioannidis, and I. Akyildiz, "End-to-end wireless path deployment with intelligent surfaces using interpretable neural networks," *IEEE Transactions on Communications*, vol. 68, no. 11, pp. 6792–6806, 2020.

[61] D. Foead, A. Ghafari, M. B. Kusuma, N. Hanafiah, and E. Gunawan, "A systematic literature review of a* pathfinding," *Procedia Computer Science*, vol. 179, pp. 507–514, 2021.

[62] C. Antoniadis, K. Katsalis, D. Tyrovolas, S. A. Tegos, S. Ioannidis, P. D. Diamantoulakis, G. K. Karagiannidis, and C. Liaskos, "Hera: A novel heuristic resource allocator for multi-sdm multi-user settings," in *2024 IEEE Conference on Standards for Communications and Networking (CSCN)*. IEEE, 2024, pp. 141–146.

[63] C. Liaskos, L. Mamatas, A. Pourdamghani, A. Tsoliariadou, S. Ioannidis, A. Pitsillides, S. Schmid, and I. F. Akyildiz, "Software-defined reconfigurable intelligent surfaces: From theory to end-to-end implementation," *Proceedings of the IEEE*, vol. 110, no. 9, pp. 1466–1493, 2022.

[64] D. Tyrovolas, D. Bozanis, S. A. Tegos, V. K. Papanikolaou, P. D. Diamantoulakis, C. K. Liaskos, R. Schober, and G. K. Karagiannidis, "Empowering programmable wireless environments with optical anchor-based positioning," *IEEE Network*, 2024.

[65] V. Loscri, C. Rizza, A. Benslimane, A. M. Vegni, E. Innocenti, and R. Giuliano, "Best-rim: A mmwave beam steering approach based on computer vision-enhanced reconfigurable intelligent metasurfaces," *IEEE Transactions on Vehicular Technology*, vol. 72, no. 6, pp. 7613–7626, 2023.

[66] M. Zhao, T. Li, M. Abu Alsheikh, Y. Tian, H. Zhao, A. Torralba, and D. Katabi, "Through-wall human pose estimation using radio signals," in *Proceedings of the IEEE conference on computer vision and pattern recognition*, 2018, pp. 7356–7365.

[67] C. Liaskos, G. Pyrialakos, A. Pitilakis, S. Abadal, A. Tsoliariadou, A. Tasolamprou, O. Tsilipakos, N. Kantartzis, S. Ioannidis, E. Alarcon *et al.*, "Absense: Sensing electromagnetic waves on metasurfaces via ambient compilation of full absorption," in *Proceedings of the Sixth Annual ACM International Conference on Nanoscale Computing and Communication*, 2019, pp. 1–6.

[68] C. Liaskos, A. Tsoliariadou, A. Pitilakis, G. Pirialakos, O. Tsilipakos, A. Tasolamprou, N. Kantartzis, S. Ioannidis, M. Kafesaki, A. Pitsillides *et al.*, "Joint compressed sensing and manipulation of wireless emissions with intelligent surfaces," in *2019 15th International Conference on Distributed Computing in Sensor Systems (DCOSS)*, 2019, pp. 318–325.

[69] C. de Lima, D. Belot, R. Berkvens, A. Bourdoux, D. Dardari, M. Guillaud, M. Isomursu, E.-S. Lohan, Y. Miao, A. N. Barreto *et al.*, "Convergent communication, sensing and localization in 6g systems: An overview of technologies, opportunities and challenges," *IEEE Access*, 2021.

[70] A. Fascista, A. Coluccia, H. Wymeersch, and G. Seco-Granados, "Ris-aided joint localization and synchronization with a single-antenna mmwave receiver," in *ICASSP 2021-2021 IEEE International Conference on Acoustics, Speech and Signal Processing (ICASSP)*, 2021, pp. 4455–4459.

[71] A. Johnston, *SIP: Understanding the session initiation protocol 2015*, 4th ed. Norwood, MA: Artech House, Oct. 2015.

[72] C. Liaskos, G. G. Pyrialakos, A. Pitilakis, A. Tsoliariadou, M. Christodoulou, N. Kantartzis, S. Ioannidis, A. Pitsillides, and I. F. Akyildiz, "Towards the internet of metamaterial things: Software enablers for user-customizable electromagnetic wave propagation," *Intelligent Reconfigurable Surfaces (IRS) for Prospective 6G Wireless Networks*, pp. 41–82, 2022.

[73] R. Campana, C. Amatetti, and A. Vanelli-Coralli, "O-ran based non-terrestrial networks: Trends and challenges," in *2023 Joint European Conference on Networks and Communications & 6G Summit (EuCNC/6G Summit)*. IEEE, 2023, pp. 264–269.

[74] Industry Specification Group (ISG) on Reconfigurable Intelligent Surfaces (RIS), "RIS — etsi.org," <https://www.etsi.org/committee/ris>, [Accessed 29-12-2025].

[75] ETSI Communications, "ETSI publishes first Report on ISAC Use Cases for 6G — etsi.org," <https://www.etsi.org/newsroom/press-releases/2520-etsi-publishes-first-report-on-isac-use-cases-for-6g>, [Accessed 29-12-2025].

[76] Industry Specification Group (ISG) on Network Function Virtualization (NFV), "NFV — etsi.org," <https://www.etsi.org/committee/1427-nfv>, [Accessed 29-12-2025].

[77] "Wireless InSite Engineered Electromagnetic Surfaces (EES) | Remcom — remcom.com," <https://www.remcom.com/wireless-insite-em-propagation-software/engineered-electromagnetic-surfaces-ees>, [Accessed 31-12-2025].

- [78] A. Papadopoulos, A. Lalas, K. Votis, D. Tyrovolas, G. Karagiannidis, S. Ioannidis, and C. Liaskos, “An open platform for simulating the physical layer of 6g communication systems with multiple intelligent surfaces,” in *2022 18th International Conference on Network and Service Management (CNSM)*. IEEE, 2022, pp. 359–363.
- [79] “Sienna Software — developer.nvidia.com,” <https://developer.nvidia.com/sienna>, [Accessed 31-12-2025].
- [80] R. Sharma, V. Vashisht, and U. Singh, “Modelling and simulation frameworks for wireless sensor networks: a comparative study,” *IET Wireless Sensor Systems*, vol. 10, no. 5, pp. 181–197, 2020.
- [81] A. Varga, “Discrete event simulation system,” in *Proc. of the European Simulation Multiconference (ESM’2001)*, vol. 17, 2001.
- [82] “GitHub 6G-simulation-platform,” <https://github.com/alexpapad95/6G-simulation-platform>, [Accessed 31-12-2025].
- [83] “GitHub Calc-ScatPat: MATLAB implementation of the Huygens-Fresnel principle for the calculation of the scattering farfield pattern produced from the illumination of a finite-aperture rectangular metasurface,” <https://github.com/alexpitii/Calc-ScatPat>, [Accessed 31-12-2025].
- [84] G. Dimopoulos, “Pwe graph generation — bsc thesis,” https://www.cse.oui.gr/~cliaskos/pwe_graphs/dimopoulosgeorgios-thesis.eu/index.html, [Accessed 31-12-2025].
- [85] Series P, “Propagation data and prediction methods for the planning of short-range outdoor radiocommunication systems and radio local area networks in the frequency range 300 mhz to 100 ghz,” *ITU recommendations*, pp. 1411–9, 2017.
- [86] Mathworks, “Wireless channel designer,” <https://www.mathworks.com/help/5g/ref/wirelesschanneldesigner-app.html>, [Accessed 31-12-2025].
- [87] Y. Li, C.-H. Lee, and J. Gao, “From computer-aided to intelligent machining: Recent advances in computer numerical control machining research,” *Proceedings of the Institution of Mechanical Engineers, Part B: Journal of Engineering Manufacture*, vol. 229, no. 7, pp. 1087–1103, 2015.
- [88] B. Agarwal, M. A. Togou, M. Marco, and G.-M. Muntean, “A comprehensive survey on radio resource management in 5g hetnets: Current solutions, future trends and open issues,” *IEEE Communications Surveys & Tutorials*, vol. 24, no. 4, pp. 2495–2534, 2022.
- [89] C. Xue, T. Zhang, Y. Zhou, M. Nixon, A. Loveless, and S. Han, “A survey and experimental study of real-time scheduling methods for 802.1 qbv tsn networks,” *ACM Computing Surveys*, 2025.
- [90] X. Zhang, H. Xing, Y. Shen, J. Xu, and S. Cui, “Age of information minimization in uav-enabled iot networks via federated reinforcement learning,” *IEEE Transactions on Wireless Communications*, 2025.
- [91] S. Mavridopoulos, P. Nicopolitidis, G. Papadimitriou, and P. Sarigiannidis, “Broadcast levels: Efficient and lightweight schedule construction for push-based data broadcasting systems,” *IEEE Transactions on Broadcasting*, vol. 61, no. 3, pp. 470–481, 2015.
- [92] J. L. Träff, “Optimal broadcast schedules in logarithmic time with applications to broadcast, reduction, all-broadcast and all-reduction,” *ACM Transactions on Parallel Computing*, 2025.
- [93] R. Iqbal, D. Bozanis, D. Tyrovolas, C. K. Liaskos, M. A. Imran, G. K. Karagiannidis, and H. Abumashoud, “Integrated localization, mapping, and communication through vcsel-based light-emitting ris (leris),” *arXiv preprint arXiv:2510.08071*, 2025.
- [94] P. Cisek, “Making decisions through a distributed consensus,” *Current opinion in neurobiology*, vol. 22, no. 6, pp. 927–936, 2012.
- [95] N. M. K. Chowdhury, M. R. Rahman, and R. Boutaba, “Virtual network embedding with coordinated node and link mapping,” in *IEEE INFOCOM 2009*. IEEE, 2009, pp. 783–791.
- [96] X. He, Z. Tu, M. Wagner, X. Xu, and Z. Wang, “Online deployment algorithms for microservice systems with complex dependencies,” *IEEE Transactions on Cloud Computing*, vol. 11, no. 2, pp. 1746–1763, 2022.
- [97] E. Tohidi, M. Franke, A. Drummond, S. Schmid, A. Jukan, and S. Stańczak, “Ris-assisted 6g networks: Challenges and tradeoffs in control standardization,” in *2024 IEEE Conference on Standards for Communications and Networking (CSCN)*. IEEE, 2024, pp. 36–41.
- [98] C. Liaskos, A. Tsoliaridou, K. Georgopoulos, I. Morianos, S. Ioannidis, I. Salem, D. Manesis, S. Schmid, D. Tyrovolas, S. A. Tegos *et al.*, “Xr-rf imaging enabled by software-defined metasurfaces and machine learning: Foundational vision, technologies and challenges,” *IEEE access*, vol. 10, pp. 119 841–119 862, 2022.
- [99] D. A. Miller, “Why optics needs thickness,” *Science*, vol. 379, no. 6627, pp. 41–45, 2023.